Theoretical Study on the Speed of Sound in a Bubbly Liquid

Junya KAWAHARA

Division of Mechanical and Space Engineering

Hokkaido University

March 1, 2016

Contents

Chapter 1

Introduction

1.1 Pressure wave propagation in a bubbly liquid

Pressure wave propagation in a bubbly liquid is important for the development of applications such as the microbubble-enhanced High Intensity Focused Ultrasound utilized in the medical field [1,2] and the sonar by an underwater sound in the marine field [3–5]. The presence of gas bubbles dispersed in a liquid affects profoundly the acoustic behaviour of the medium. For example, the dispersion is caused by bubble oscillations in a bubbly liquid, in which waves of different wavelength propagate with different phase speeds [6, 7]. The reduction in the speed of sound is also well known [8–10]. In this section, we will review previous theoretical studies on pressure wave propagation in a bubbly liquid.

Pressure waves propagating in a bubbly liquid cause oscillations of bubbles in the medium [Fig. 1.1(a)]. A number of investigators had studied the single bubble oscillation [12–24]. The dynamics of several bubbles had been also studied, where bubble-bubble interactions are taken into account. Shima [25], Morioka [26], Wraith & Kakutami [27], and Fujikawa & Takahira [28] studied the dynamics of two bubbles in an incompressible liquid. Takahira *et al.* [29,30] formulated a mathematical model

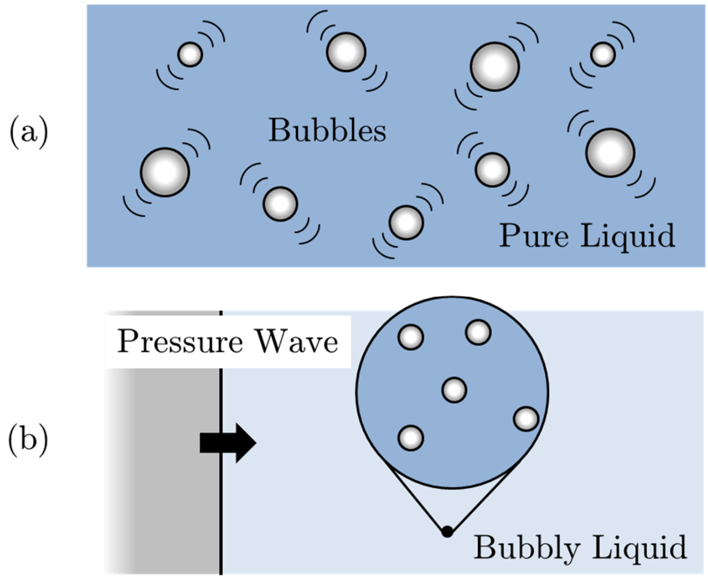

Figure 1.1: (a) The oscillation of individual bubble in a bubble cluster, which consist of an arbitrary number of bubble, is investigated by using the theoretical model for the bubble dynamics. (b) Pressure wave propagation in a bubbly liquid, which contains numerous bubbles, has been investigated based on the averaging method [11]. Here, the bubbly liquid is assumed to be a homogeneous continuum medium.

for the dynamics of multiple bubbles in an incompressible liquid. Takahira *et al.* [31] numerically investigated the influence of bubble-bubble interactions on collapse motions of a bubble cluster by using their model. Watanabe & Prosperetti [32] derived a mathematical model describing the acoustical characteristics of a bubble cloud containing multiple bubbles taking the influence of bubble-bubble interactions into account. Watanabe & Prosperetti [33] explored the validity of the continuum model for a bubbly liquid by using their model. Based on Fujikawa & Takahira [28] and Takahira *et al.* [29], Egashira *et al.* [34] theoretically investigated the influence of bubble-bubble interactions on the added mass of a bubble cluster in an incompressible liquid. Fujikawa & Takahira [35] theoretically studied the interaction between two spherical bubbles and radiated pressure waves with a consideration of the liquid compressibility. They formulated a mathematical model for the radial oscillation of two spherical bubbles in a compressible liquid. By using this model, Takahira *et* *al.* [36] numerically investigated nonlinear oscillations of two spherical bubbles in a compressible liquid. The mathematical model for two spherical bubbles in a compressible liquid was extended to the case of multiple bubbles by Takahira *et al.* [37]. Konno *et al.* [38] simulated the oscillations of multiple bubbles placed near a rigid wall by using the mathematical model in Ref. [37].

Above studies focused on the dynamics of individual bubbles in a bubble cluster, which consists of an arbitrary number of bubbles [Fig. 1.1(a)]. However, when numerous bubbles are contained in a liquid, the investigation of all the dynamics of individual bubbles in the bubbly liquid is difficult; then, pressure wave propagation in the bubbly liquid has been investigated based on the averaging method [11] [Fig. 1.1(b)]. Around fifty years ago, van Wijngaarden conducted pioneering studies on pressure wave propagation in a bubbly liquid [39–41]. He formulated averaged conservation laws for bubbly flows based on heuristic reasoning. Caflisch *et al.* [42] derived a system of effective equations for wave propagation in a bubbly liquid by using Foldy's approximation [7]. Commander & Prosperetti [43] reviewed the theoretical models derived by van Wijngaarden [39] and Caflisch *et al.* [42], and compared the dispersion relation with experimental data. Zhang & Prosperetti [44] derived a system of averaged equations for a bubbly flow by using the ensemble averaging method introduced in Ref. [45]. Watanabe & Prosperetti [46] theoretically studied weak shock propagation in a bubbly liquid on the basis of a mathematical model derived by Caflisch *et al.* [42]. They pointed out the importance of the thermal exchange between the gas bubbles and the liquid. Egashira *et al.* [47, 48] proposed a two-fluid model equation for a bubbly flow. They theoretically and numerically investigated linear pressure wave propagation in a bubbly liquid by using this model. Colonius *et al.* [49] proved the existence of the statistical equilibrium of bubble oscillation in a bubbly flow due to phase cancellations among bubbles with different sizes. Ando *et al.* [50] derived a continuum bubbly flow model that incorporates a distribution of equilibrium bubble nuclei sizes, and quantified the influence of polydispersity on averaged shock dynamics. Kanagawa *et al.* [51–54] proposed a systematic derivation method of the nonlinear wave equations in a bubbly liquid on the basis of appropriate choices of scaling relations of physical parameters. Fuster & Colonius [55] proposed volume-averaged equations incorporating a subgrid model which governs the dynamics of multiple bubbles. Fuster *et al.* [56] studied the influence of bubble-bubble interactions on linear pressure wave propagation in a bubbly liquid by using the model proposed in Ref. [55].

1.2 Speed of sound in a bubbly liquid

Pressure wave propagation in a liquid containing bubbles in a duct is important for the development of mechanical engineering applications [57–66]. Recently, Kaneko *et al.* proposed a technique to generate microbubbles utilizing a venturi tube [67,68]. They explained the mechanism of microbubble generation in a venturi tube based on a well-known theory of supersonic flow in a Laval nozzle. Because the speed of sound in a bubbly liquid is much lower than that in a pure liquid, the velocity of a bubbly flow easily reaches the speed of sound in a bubbly liquid in the throat of a venturi tube. Subsequently, with the rapid pressure recovery in the diverging area, several or a few bubbles injected into the converging area collapse violently in the diverging area. The collapse of these bubbles generates numerous microbubbles in the diverging area. The mechanism of microbubble generation can be explained on the basis of the reduction in the speed of sound in the liquid containing bubbles.

The addition of even a small number of air bubbles, representing as little as 0.01% by volume, into water can reduce the speed of sound in the water by about 40% [69]. In the classic paper of Mallock [70], an approximate expression for the speed of sound was obtained in a liquid containing bubbles, in which a homogeneous

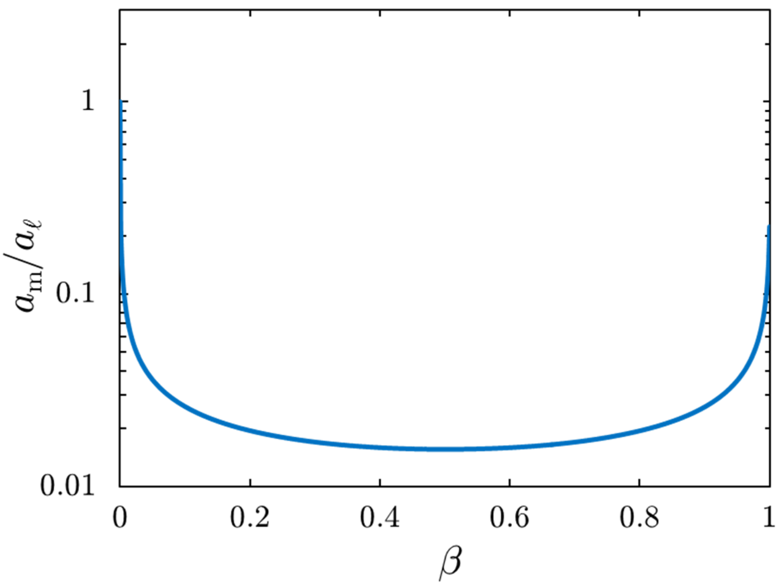

Figure 1.2: Speed of sound in a mixture of liquid and gas given by Wood's equation [69] with $\rho_\ell = 998.2$ kg/m^3, $\rho_{\mathrm{g}} = 1.21$ kg/m^3, $a_\ell = 1483$ m/s, $a_{\mathrm{g}} = 333$ m/s.

medium can be assumed. Wood [69] confirmed Mallock's study, and formulated the more practical form of the speed of sound in a mixture of two fluid media. A number of investigators [40, 71–74] reviewed the speed of sound in a bubbly liquid.

In previous studies shown in this section and Section 1.1, the mechanism of the reduction in the speed of sound was explained in a bubbly liquid, in which a homogeneous medium could be assumed. In general, the speed of sound a is defined as $a = 1/\sqrt{\rho\kappa}$, where ρ is the density and κ is the compressibility [71, 72, 75]; therefore, we need to derive these quantities for a bubbly liquid. The most important parameter is the volume fraction of the gas phase, i.e., the void fraction β that is given by $\beta = V_{\mathrm{g}}/(V_\ell + V_{\mathrm{g}})$, where V is the volume and the subscripts ℓ and g refer to the liquid and gas phases, respectively. The mixture density and compressibility are $\rho_{\mathrm{m}} = (1-\beta)\rho_\ell + \beta\rho_{\mathrm{g}}$ and $\kappa_{\mathrm{m}} = (1-\beta)\kappa_\ell + \beta\kappa_{\mathrm{g}}$, respectively, where the subscript m denotes the effective quantities pertaining to the mixture. Therefore, the ratio of the speed of sound in a pure liquid to that in a mixture, χ, can be written as follows:

$$\chi = \frac{a_\ell}{a_\mathrm{m}} = \left[(1-\beta)^2 + \frac{\beta^2 a_\ell^2}{a_\mathrm{g}^2} + \beta(1-\beta)\frac{\rho_\mathrm{g}^2 a_\mathrm{g}^2 + \rho_\ell^2 a_\ell^2}{\rho_\ell \rho_\mathrm{g} a_\mathrm{g}^2}\right]^{1/2}. \tag{1.2.1}$$

Equation (1.2.1) is known as Wood's equation [40, 69, 74]. Figure 1.2 shows the reduction in the speed of sound given by Wood's equation. From Eq. (1.2.1), the mechanism by which the speed of sound in a bubbly liquid is reduced from that in a pure liquid in the context of a homogeneous continuum medium can be explained. Bubbles greatly increase the mixture compressibility, but hardly affect the density. High compressibility and density yield a low speed of sound.

1.3 Purpose of this study

Recent numerical [76–80] and experimental [74, 78, 81, 82] results show that Wood's equation and the acoustic characteristics attributed to it appear to be valid even for non-homogeneous media such as a liquid containing several bubbles in a duct. These results raise a fundamental question: *Why can Wood's equation work for a liquid containing several or a few bubbles in a duct, in which a homogeneous medium can no longer be assumed?* Is it merely a coincidence? The purpose of this study is to answer this question by presenting a theoretical basis for the reduction in the speed of sound in a liquid containing gas bubbles that cannot be considered as a homogeneous continuum medium. We investigate pressure wave propagation in a bubbly liquid that is composed of spherical gas bubbles suspended in a liquid medium in a square duct. Pressure waves cause radial oscillations of the spherical gas bubbles, which generate pressure fields. Therefore, the pressure waves are scattered by the bubbles. We assume that the bubble size is much smaller than the wavelength of the pressure wave; therefore, we restrict ourselves to *low-frequency* wave propagation in a bubbly liquid [74]. Then, the bubbles become acoustic scatterers that exhibit a low-frequency resonance, known as the Minnaert resonance [83]. A number of investigators have studied pressure wave propagation including acoustic scattering generated by bubbles in a bubbly liquid, in which a homogeneous medium can be practically assumed [6, 7, 42, 43, 56, 84]. Based on their studies, we will construct a systematic theoretical model for pressure wave propagation in a duct containing a finite number of bubbles. By using this model, we will clarify the mechanism of the reduction in the speed of sound in a liquid containing bubbles in a square duct.

Recall that the speed of electric waves in a material with a refractive index n is c/n, where c is the speed of light. We were greatly inspired by the explanation of this phenomenon given in *"The Origin of the Refractive Index"* by Feynman *et al.* [85]. We can have the same discussion for the origin of χ as was given for n; therefore, we will hereafter refer to χ as the refractive index of a bubbly liquid. Recently, Leroy *et al.* [86] experimentally and theoretically studied the transmission of ultrasound through a single layer of bubbles based on Feynman's study. In this study, we will investigate pressure wave propagation in a liquid containing spherical bubbles in a square duct instead of electric wave propagation in a material.

1.4 Feynman's regime

In this study, we discuss the reduction in the speed of sound by analogy with the reduction in the speed of light. It is well known that electric waves propagate at the speed of c/n through a material whose refractive index is n. Feynman *et al.* [85] examined electric wave propagation in the material under some physical assumptions:

- *That the total electric field in any physical circumstance can always be represented by the sum of the fields from all the charges in the universe.*

- *That the field from a single charge is given by its acceleration evaluated with a retardation at the speed* c*, always (for the radiation field).*

Based on these assumptions, they explained how the material reduce the speed of light.

In a bubbly liquid, bubbles suspended in a liquid medium play roles as acoustic scatterers. A number of investigators have investigated the acoustic scattering in a bubbly liquid [43]. Recently, Leroy *et al.* [86] investigated the transmission of ultrasound through a single layer of bubbles, based on Feynman's study.

Getting inspired by their studies, we discuss pressure wave propagation in a square duct filled with a liquid that contains several bubbles under the following assumptions:

1. the flow field in the liquid is a potential flow,

2. the flow field in the liquid is described by a linear wave equation,

3. all attenuations are ignored.

We use these assumptions to investigate the oscillations of bubbles and a pressure field, as opposed to the motions of charges and an electric field in Feynman's study. Therefore, the following assumptions are made (Fig. 1.3):

- the total pressure field can always be represented by the summation of the pressure fields generated by the input pressure wave and the oscillations of all the bubbles,

- the pressure field generated by a single bubble is given by its oscillation evaluated with retardation at the speed of sound in a pure liquid.

We use a term, *Feynman's regime*, to refer to these physical assumptions.

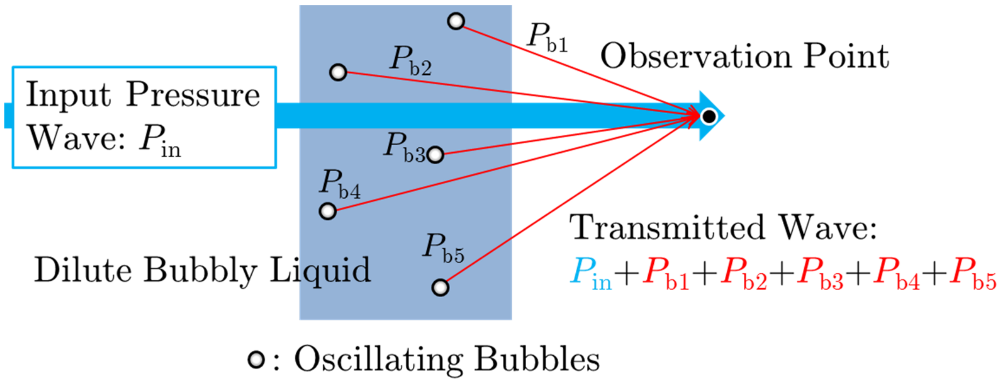

Figure 1.3: The transmitted wave, which passed through a dilute bubbly liquid, is calculated by the summation of the pressure fields generated by the input pressure wave and all the bubble oscillations.

Feynman's study [85] can be applied for electric wave propagation in the material, in which charges are distributed randomly. In this study, to construct the most fundamental and effective model, we will focus on pressure wave propagation in the duct containing in-line bubbles. Although the formulation in this thesis is designed to treat a specific problem, our study based on Feynman's regime can make a contribution to the development of general acoustics that includes statistical studies on a bubbly liquid that contains bubbles distributed randomly.

1.5 Contents of this thesis

The contents of this thesis are as follows. In Chapter 2, we theoretically investigate pressure wave propagation in a square duct containing spherical bubbles. We will clarify the fundamental mechanism of the reduction in the speed of sound in a bubbly liquid, in which a homogeneous medium can no longer be assumed. In Chapter 3, we numerically investigate pressure wave propagation in a square duct containing a finite number of bubbles. We will discuss the roles of the bubble-bubble interactions, the delay times, and the number of bubbles in the reduction in the speed of sound. In Chapter 4, we theoretically investigate pressure wave propagation in a square duct containing a single bubble affected by reflected waves from the rigid walls of the duct. We will construct the theoretical model for the phase speed of the total pressure wave in the duct. Chapter 5 is devoted to conclusions.

Chapter 2

How do bubbles reduce the speed of sound?

We theoretically investigate pressure wave propagation in a liquid containing spherical bubbles in a square duct, based on Feynman's regime. In this chapter, we will clarify the fundamental mechanism of the reduction in the speed of sound in a bubbly liquid.

2.1 Problem statement

We investigate pressure wave propagation in a square duct with sides of length D [Fig. 2.1(a)] filled with a compressible liquid that contains a single bubble placed at point B. The input plane linear wave propagates in the x direction through the duct. We measure the input plane pressure wave $p_0 + P_{\mathrm{in}}(t)$ at the center of the bubble, where t is the time, p_0 is the undisturbed pressure, and $P_{\mathrm{in}}(t)$ is the oscillatory component of the input wave. The input plane wave has an angular frequency ω and a wavelength λ, where $\omega\lambda = 2\pi a_\ell$, and has the following form: $p_0 + P_{\mathrm{in}}(t) = p_0 + P_0 \mathrm{e}^{\mathrm{i}\omega t}$, where P_0 is the amplitude of the input wave ($P_0/p_0 \ll 1$).

(a)

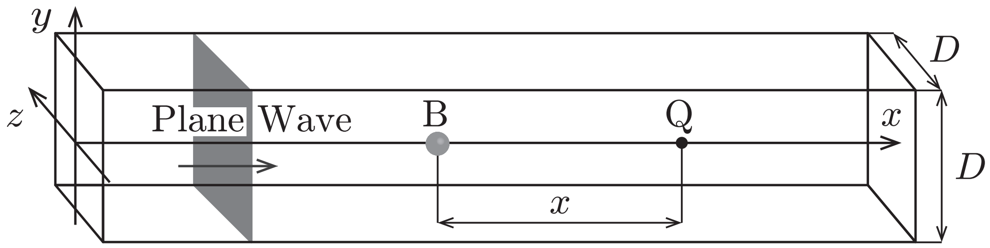

(b)

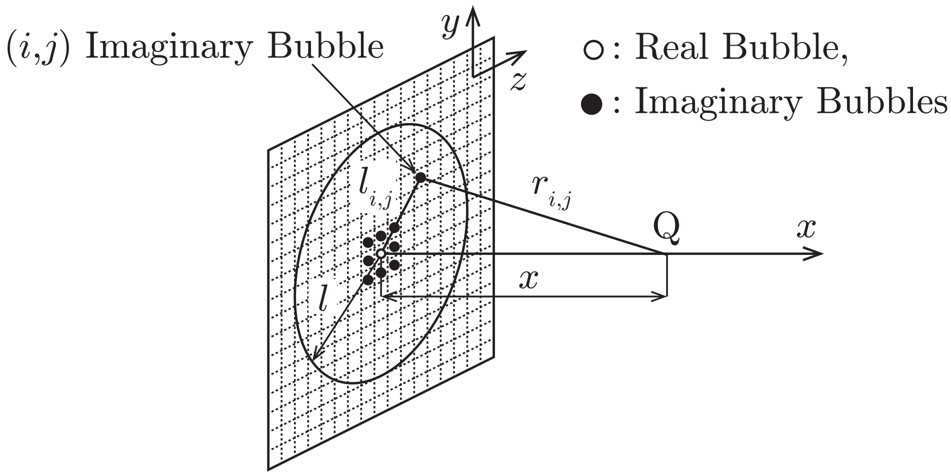

Figure 2.1: (a) Single spherical bubble placed in a square duct filled with a compressible liquid. (b) Schematic of the distribution of imaginary bubbles in the $y - z$ plane.

Now, we will consider the pressure field generated at point Q by the radial oscillation of a spherical bubble. In this study, the following assumptions are made:

(i). the center of a bubble is fixed in the duct,

(ii). the radial oscillation of a bubble is spherically symmetric,

(iii). a bubble is initially at rest,

(iv). the terms of the attenuation due to the acoustic radiation of order $1/a_\ell$ are neglected.

Then, the liquid velocity potential φ for the flow field generated by the radial oscillation of a single bubble at the distance r can be written as $\varphi(t) = -R^2(t-r/a_\ell)\dot{R}(t-r/a_\ell)/r$ [17,19,35,37,87], where $R(t)$ is the bubble radius. It should be emphasized here that all attenuations, including the acoustic radiation of order $1/a_\ell$, are ignored; however, the delay time is considered (where the delay time is defined as the finite amount of time that it takes for a pressure wave to propagate a given distance with the speed of sound in a pure liquid). We further assume that the bubble is filled with a non-condensable gas that follows the polytropic process without phase changes; then, the radial oscillation of the bubble is given by Refs. [12,19,88],

$$R(t)\ddot{R}(t) + \frac{3}{2}\dot{R}^2(t) = \frac{1}{\rho_\ell}\left\{p_0\left[\frac{R_0}{R(t)}\right]^{3\gamma} - p_{\mathrm{v}}(t)\right\}, \tag{2.1.1}$$

where R_0 is the initial undisturbed bubble radius, γ is the polytropic constant, and $p_{\mathrm{v}}(t)$ is defined as the pressure in the liquid at the location of the bubble center in the absence of the bubble [19]. By substituting $p_0 + P_{\mathrm{in}}(t)$ into $p_{\mathrm{v}}(t)$, we linearize Eq. (2.1.1),

$$\ddot{R}'(t) + \omega_0^2 R'(t) = -\frac{P_{\mathrm{in}}(t)}{\rho_\ell R_0}, \tag{2.1.2}$$

where $R'(t)$ is the small fluctuation of the bubble radius: $R'(t) = R(t) - R_0$ ($|R'|/R_0 \ll 1$) and ω_0 is the natural angular frequency of the bubble: $\omega_0 = \sqrt{3\gamma p_0/(\rho_\ell R_0^2)}$ ($\omega/\omega_0 \ll 1$). By solving Eq. (2.1.2), we can write $R'(t)$ as a function of time: $R'(t) = -s_0 e^{i\omega t}$, where $s_0 = P_0/\left[\rho_\ell R_0 \left(\omega_0^2 - \omega^2\right)\right]$. Note that the pressure field generated at Q at the instant t is given by the radial oscillation of the bubble at the earlier time $t' = t - x/a_\ell$, where x/a_ℓ is the time it takes for the pressure wave to propagate the distance x from the point B to the point Q. We can calculate the pressure field generated at Q by using the following equation:

$$P_{\mathrm{b}}(t) = -\rho_\ell \left[\frac{\partial \varphi(t)}{\partial t}\right] = \rho_\ell R_0^2 \frac{\omega^2 s_0 e^{i\omega(t - x/a_\ell)}}{x}. \tag{2.1.3}$$

The radiative wave generated by the bubble is reflected off the rigid walls of the duct. The boundary condition on the rigid walls can be written as follows:

$$\frac{\partial \Phi}{\partial w} = 0, \tag{2.1.4}$$

where Φ is the liquid velocity potential for the total flow field and $\partial/\partial w$ is the normal derivative on the rigid walls. We determine the reflected wave by calculating the pressure field due to the oscillations of imaginary bubbles, i.e., by using the method of images [89–91]. We place an infinite number of imaginary bubbles into a two-dimensional array in the $y - z$ plane; therefore, we investigate a layer of bubbles [86,92–96] as shown in Fig. 2.1(b). We only consider the case of a duct with a sufficiently large D. That is to say, we impose the following assumption:

(v). the number density of bubbles in the $y - z$ plane, η, which is defined as $\eta = D^{-2}$, is very close to 0.

We use this assumption to avoid $p_{\mathrm{v}}(t)$ being modified by contributions from imaginary bubbles.

2.2 Pressure field generated by a single bubble in a square duct

We can find the total pressure field by adding the pressure fields generated by the real and imaginary bubbles. We observe the pressure field only at finite x and t; therefore, we need to add the contributions from the bubbles within a circle of radius l from B in the $y-z$ plane, as shown in Fig. 2.1(b), where $l^2 = (a_\ell t)^2 - x^2$. We define the summation of the pressure fields generated by these bubbles as P_{bs}. The total pressure field generated at Q is given as the summation of P_{in} and P_{bs} [35,37,55,56]:

$$P_{\mathrm{tot}}(t) = P_0 \mathrm{e}^{\mathrm{i}\omega(t-x/a_\ell)} + \sum_{i,j(l_{i,j}<l)} \rho_\ell R_0^2 \frac{\omega^2 s_0 \mathrm{e}^{\mathrm{i}\omega(t-r_{i,j}/a_\ell)}}{r_{i,j}}, \tag{2.2.1}$$

where $l_{i,j}$ is the distance from the point B to the center of the (i,j) imaginary bubble and $r_{i,j}^2 = x^2 + l_{i,j}^2$. The second term in the right-hand side of Eq. (2.2.1) represents P_{bs}. Because the delay time $r_{i,j}/a_\ell$ varies in accordance with the change of $r_{i,j}$, the pressure field generated by each bubble is out of phase each other. Here, we qualitatively discuss the summation of the pressure fields having the phase shifts, based on Refs. [85,97]. In the layer of bubbles, we consider concentric circles whose center is the point B [Fig. 2.2(a)]. The distance between the point Q and any point on the circumference of the n-th circle is $x + n\delta r$, where $\delta r \ll x$. We define the doughnut-shaped area enclosed by the n-th and $(n+1)$-th circle as $S_{(n)}$. The area $S_{(n)}$ can be written as

$$\begin{aligned} S_{(n)} = \pi l_{(n+1)}^2 - \pi l_{(n)}^2 &= \pi \left\{ [x + (n+1)\delta r]^2 - (x + n\delta r)^2 \right\} \\ &= \pi \left[2\delta r x + (2n+1)\delta r^2 \right], \end{aligned} \tag{2.2.2}$$

where $l_{(n)} = \sqrt{(x+n\delta r)^2 - x^2}$. The number of bubbles in $S_{(n)}$ is given by $\eta S_{(n)}$. We define the summation of the pressure fields generated by the bubbles in $S_{(n)}$ as $P_{(n)}$. The amplitude of $P_{(n)}$, $|P_{(n)}|$, can be written by

$$|P_{(n)}| = \rho_\ell R_0^2 \omega^2 s_0 \eta \frac{S_{(n)}}{x+n\delta r}, \tag{2.2.3}$$

where the distance between the point Q and the bubbles in $S_{(n)}$ is assumed to be $x + n\delta r$. Note that ρ_ℓ, R_0, ω, s_0, and η are constants; hence, $|P_{(n)}|$ depends on $S_{(n)}/(x+n\delta r)$. Here, $S_{(n)}/(x+n\delta r)$ is written as following:

$$\frac{S_{(n)}}{x+n\delta r} = \pi x \frac{2\epsilon/n + (2+1/n)\epsilon^2}{1/n + \epsilon}, \tag{2.2.4}$$

where $\epsilon = \delta r/x \ll 1$. In the limit as $n \to \infty$, $S_{(n)}/(x+n\delta r) \to 2\pi\delta r$. Furthermore, in the limit as $\delta r \to 0$, $S_{(n)}/(x+n\delta r) \to 0$. Therefore, $|P_{(n)}|$ decreases in accordance with the increase of the path $x+n\delta r$ which is the distance between the point Q and the area $S_{(n)}$.

Next, we examine the summation of the pressure field generated by the bubbles in each area. The delay time that it takes for $P_{(n)}$ to propagate to the point Q is $(x+n\delta r)/a_\ell$; therefore, the phase shift σ between $P_{(n)}$ and $P_{(n+1)}$ is written as $\omega\delta r/a_\ell$. Now, we geometrically examine the summation of the pressure fields having the phase shifts by using Fig. 2.2(b). The n-th vector in Fig. 2.2(b) represents $P_{(n)}$, where the length of this vector is $|P_{(n)}|$, and the angle between this vector and the real axis is the phase of $P_{(n)}$. The summation of the pressure fields generated by the bubbles within the circle of radius l_1 is $P_{(0)}$. We suppose that the angle between the vector $P_{(0)}$ and the real axis is 0, and the vector $P_{(0)}$ directs to the positive direction. The angle between the vector $P_{(0)}$ and $P_{(n)}$ is the phase shift $\omega n\delta r/a_\ell$ caused by the path different. Because the wave propagation distance $a_\ell t$ increases with the lapse of time, we need to consider the pressure fields generated by bubbles in farther areas. The phases of these pressure fields deviate from each other depending on the path difference. If these pressure fields have the same amplitude, P_{bs} periodically changes with drawing a circular orbit while the phase of P_{bs} is shifted by σ. Actually, because $|P_{(n)}|$ (the length of the vector) decreases in accordance with the increase of the path, P_{bs} converges at the center of the circle with drawing the spiral orbit, as shown Fig. 2.2(b). A simple geometry gives the following expression for the center of the circle:

$$\mathrm{i}\frac{|P_{(0)}|}{\sigma} = \mathrm{i}\omega\left(2\pi a_\ell \rho_\ell R_0^2 \eta\right) s_0, \tag{2.2.5}$$

where $\delta r \to 0$. Therefore, when the enough time for P_{bs} to converge has passed, we can calculate the total pressure field as follows:

$$P_{\mathrm{tot}}(t) = (1 - \mathrm{i}\Delta\theta) P_0 \mathrm{e}^{\mathrm{i}\omega(t - x/a_\ell)} \simeq P_0 \mathrm{e}^{-\mathrm{i}\Delta\theta} \mathrm{e}^{\mathrm{i}\omega(t - x/a_\ell)}, \tag{2.2.6}$$

with

$$\Delta\theta = \omega\left(\frac{2\pi a_\ell R_0 \eta}{\omega_0^2 - \omega^2}\right) \ll 1. \tag{2.2.7}$$

The most important term in this study is $\mathrm{e}^{-\mathrm{i}\Delta\theta}$. As Feynman *et al.* [85] stated: multiplying an oscillating function $\mathrm{e}^{\mathrm{i}\omega t}$ by a factor $\mathrm{e}^{-\mathrm{i}\Delta\theta}$ is equivalent to changing the phase of the oscillation by the angle $-\Delta\theta$. This retards the phase by the amount $\Delta\theta$, i.e., $\omega\left[2\pi a_\ell R_0 \eta/(\omega_0^2 - \omega^2)\right]$.

2.3 Mechanism of the reduction in the speed of sound

We further consider this phase delay by using Fig. 2.3(a). The solid (blue) curve in Fig. 2.3(a) represents P_{in}. This input pressure wave oscillates the bubble, generating

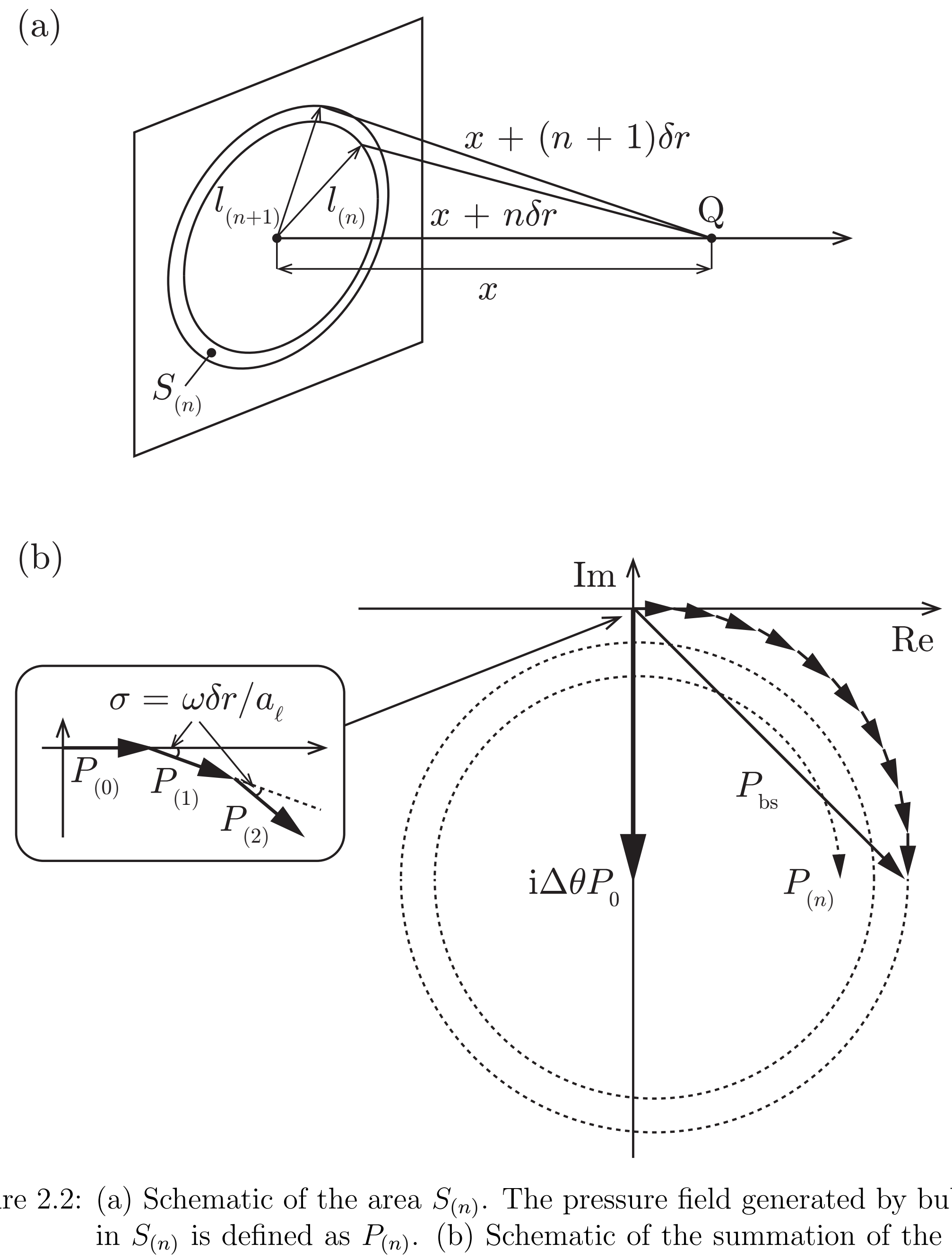

Figure 2.2: (a) Schematic of the area $S_{(n)}$. The pressure field generated by bubbles in $S_{(n)}$ is defined as $P_{(n)}$. (b) Schematic of the summation of the pressure fields having the phase shifts caused by the path difference. The summation of the pressure fields converges with drawing the spiral orbit.

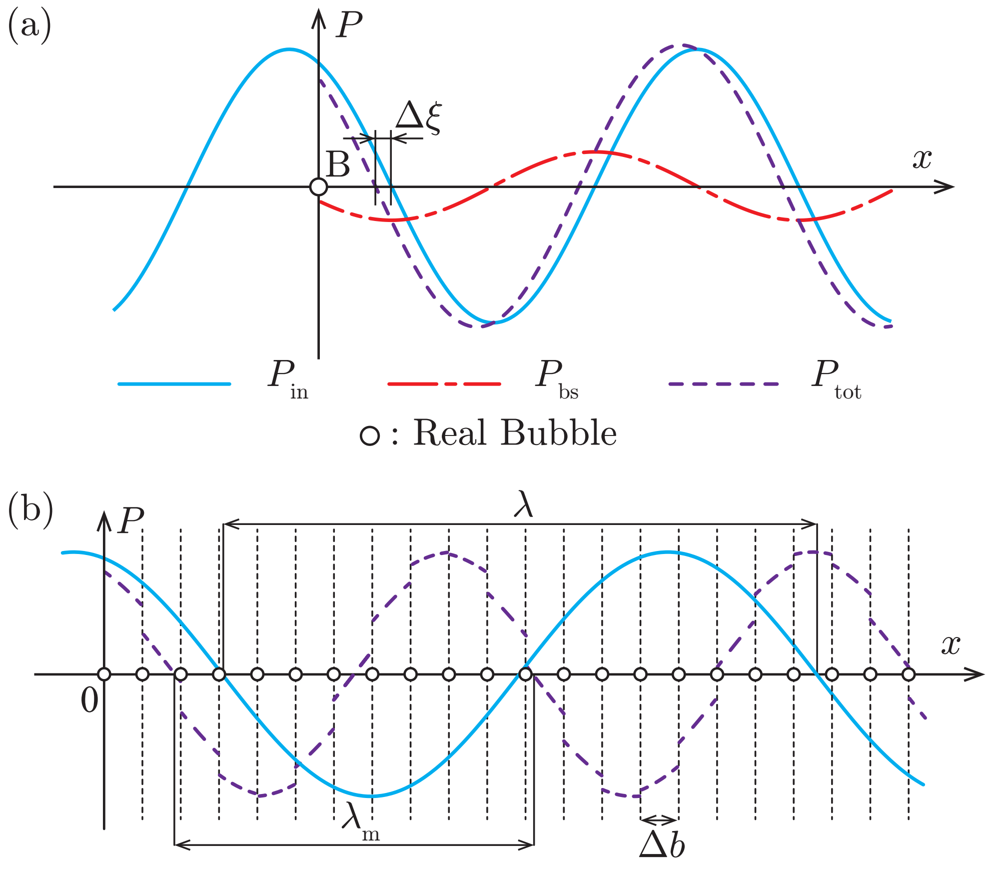

Figure 2.3: (a) The input pressure wave is modified by the pressure wave generated by the real and imaginary bubbles with the delay distance $\Delta\xi$. (b) The reduction of the wavelength due to the delay distance is caused by the induced oscillation of multiple bubbles.

$P_{\rm bs}$ [the chain (red) curve]. This generated wave $P_{\rm bs}$ has a phase delay of $\pi/2$. Only the propagating wave in the positive x direction is drawn in Fig. 2.3(a). The dashed (purple) curve is the superposition of the solid and chain curves, $P_{\rm tot}$. The total pressure wave is *delayed* in space by $\Delta\xi$, as shown in Fig. 2.3(a). The delay distance $\Delta\xi$ is related to the phase delay $\Delta\theta$ as follows:

$$\Delta\xi = \frac{\lambda}{2\pi}\Delta\theta. \tag{2.3.1}$$

Once a_ℓ, R_0, η, ω, and ω_0 are determined, $\Delta\xi$ can be calculated as a constant; therefore, $\Delta\xi$ is independent of x and t.

We investigate the role of $\Delta\xi$ in the reduction in the speed of sound in a liquid containing a large number of bubbles to determine whether our model can derive Eq. (1.2.1). We suppose that a large number of bubbles are evenly aligned along the center-line of the square duct with a separation of Δb, as shown in Fig. 2.3(b). Here, we impose the following assumption:

(vi). the distance between bubbles is sufficiently large so that the bubble-bubble interactions do not appear.

We will now discuss the wavelength of the total pressure wave in the media. The wavelength is defined as the distance between consecutive corresponding points of the same phase. The wavelength of the input pressure wave, λ, is shown in Fig. 2.3(b). Figure 2.3(b) illustrates that the delay distance $\Delta\xi$ causes a reduction in the wavelength; namely, the apparent wavelength of the total pressure wave, $\lambda_{\rm m}$, is less than λ. The angular frequency of the total pressure wave has the same angular frequency as the input pressure wave; this can be understood from Eqs. (2.2.1) and (2.2.6). Therefore, $\lambda_{\rm m} < \lambda$ leads to the result that $a_{\rm m} < a_\ell$ because $a_{\rm m} = \omega\lambda_{\rm m}/(2\pi)$. This is the fundamental mechanism of the apparent reduction in the speed of sound in a bubbly liquid. In this study inspired by Feynman *et al.* [85], the phase speed of the total pressure wave is the speed of sound in a bubbly liquid.

Let us examine the apparent wavelength of the total pressure wave, λ_{m}. Suppose that the first bubble [the leftmost bubble in Fig. 2.3(b)] is placed at the origin; then, the x-coordinate of the k-th bubble, x_k, is $(k-1)\Delta b$. We can elaborate on how these k bubbles reduce the wave propagation distance as defined by the product of the wavelength and the number of waves. We set the reference point at $-\Delta x_{\mathrm{L}}$, where $0 < \Delta x_{\mathrm{L}} < \Delta b$, to avoid phase discontinuity at the origin. Then, we adopt the distance from $-\Delta x_{\mathrm{L}}$ to $x_k + \Delta x_{\mathrm{R}}$ as the wave propagation distance of the total pressure wave, d_{m}, where $0 < \Delta x_{\mathrm{R}} < \Delta b$: $d_{\mathrm{m}} = \Delta x_{\mathrm{L}} + \Delta x_{\mathrm{R}} + (k-1)\Delta b$. The difference between d_{m} and the wave propagation distance of the input pressure wave, d, is the summation of the delay distances caused by the k bubbles. Therefore, $d = d_{\mathrm{m}} + k\Delta\xi$, which can be understood graphically from Figs. 2.3(a) and (b). Now, we introduce the most essential assumption that $k \gg 1$; then, the refractive index of the bubbly liquid, χ_{m}, can be obtained from the following:

$$\chi_{\mathrm{m}} = \frac{a_\ell}{a_{\mathrm{m}}} = \frac{\lambda}{\lambda_{\mathrm{m}}} = \frac{d}{d_{\mathrm{m}}} = 1 + \frac{k}{\Delta x_{\mathrm{L}} + \Delta x_{\mathrm{R}} + (k-1)\Delta b}\left(\frac{\lambda\Delta\theta}{2\pi}\right) \simeq 1 + \frac{\lambda\Delta\theta}{2\pi\Delta b} > 1. \tag{2.3.2}$$

The volume fraction of bubbles, β_{m}, is formally given as

$$\beta_{\mathrm{m}} = \frac{4\pi\eta R_0^3}{3\Delta b}. \tag{2.3.3}$$

Then, with the use of Eq. (2.2.7), Eq. (2.3.2) can be rewritten as follows:

$$\chi_{\mathrm{m}} = 1 + \frac{\omega\lambda}{2\pi\Delta b}\left(\frac{2\pi a_\ell R_0\eta}{\omega_0^2 - \omega^2}\right) \simeq 1 + \frac{1}{2}\frac{\rho_\ell a_\ell^2}{p_0}\beta_{\mathrm{m}}, \tag{2.3.4}$$

where the conditions $\omega \ll \omega_0$ and $\gamma = 1$ are used. The right-hand side of Eq. (2.3.4) can be also derived from Eq. (1.2.1) when the relation $p_0 = \rho_{\mathrm{g}} a_{\mathrm{g}}^2$ is used and the conditions $\beta \ll (\rho_{\mathrm{g}} a_{\mathrm{g}}^2)/(\rho_\ell a_\ell^2) \ll 1$ are imposed in Eq. (1.2.1).

Now, we obtain the most remarkable result that the refractive index of a bubbly liquid [Eq. (2.3.4), which has been well-validated experimentally] can be derived from the phase delay caused by radial oscillations of numerous bubbles aligned in the square duct. This result clearly shows that the phase delay caused by bubble oscillations is the essential physical process that contributes to the reduction in the speed of sound in a bubbly liquid in a duct. The role of bubble oscillations in the reduction in the speed of sound is qualitatively the same as that of electron oscillations in the reduction in the speed of light in a material with a refractive index of $n > 1$.

2.4 Can a single bubble reduce the speed of sound in a square duct?

Now, we are ready to discuss the following: *Can a single bubble reduce the speed of sound in a square duct?* We consider a liquid volume whose length is Δx. By substituting $k = 1$ and $\Delta x_{\mathrm{L}} = \Delta x_{\mathrm{R}} = \Delta x/2$ into Eq. (2.3.2), we obtain the refractive index of the liquid volume that contains a single bubble, χ_{s}, which is also the ratio of the speed of sound in a pure liquid to that in the liquid volume that contains just one bubble:

$$(\chi_{\mathrm{s}} - 1)\,\Delta x = \frac{\lambda \Delta\theta}{2\pi}. \tag{2.4.1}$$

The right-hand side of Eq. (2.4.1) is a well-defined positive constant, where $\Delta\theta$ can be calculated using Eq. (2.2.7); therefore, $\chi_{\mathrm{s}} > 1$. This result, $\chi_{\mathrm{s}} > 1$, shows that just one bubble can reduce the speed of sound in a square duct.

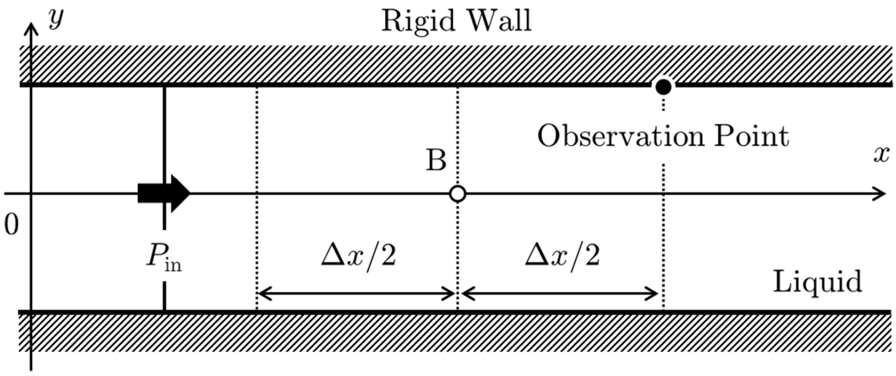

Figure 2.4: Schematic of the $x-y$ plane of the computational domain.

2.4.1 Numerical simulation

To validate Eq. (2.4.1), we numerically investigate linear pressure wave propagation in a square duct containing a single bubble (Fig. 2.4). The input plane wave starts to propagate from $x = 0$. We perform the simulations under the assumptions in this chapter except the assumption (v); therefore, the pressure in the liquid, $p_{\mathrm{v}}(t)$, is modified by the pressure fields generated by the imaginary bubbles. Then, $p_{\mathrm{v}}(t)$ is rewritten as follows:

$$p_{\mathrm{v}}(t) = p_0 + P_{\mathrm{in}}(t) + \sum_{i,j(l_{i,j}<a_\ell t)} \rho_\ell R_0^2 \frac{\ddot{R}'(t - l_{i,j}/a_\ell)}{l_{i,j}}, \tag{2.4.2}$$

where the third term in the right-hand side of Eq. (2.4.2) represents the summation of the pressure fields generated by the imaginary bubbles. By substituting Eq. (2.4.2) into Eq. (2.1.1), we can obtain the following equation:

$$\ddot{R}'(t) + \omega_0^2 R'(t) = -\frac{P_{\mathrm{in}}(t)}{\rho_\ell R_0} - \sum_{i,j(l_{i,j}<a_\ell t)} R_0 \frac{\ddot{R}'(t - l_{i,j}/a_\ell)}{l_{i,j}}. \tag{2.4.3}$$

We numerically calculate $R(t)$ affected by reflected waves by using Eq. (2.4.3).

Now, we numerically calculate the total pressure field in the duct. The total pressure field P_{tot} is given as the summation of P_{in} and the pressure fields generated

Table 2.1: Numerical conditions (in a water at 20°C).

Undisturbed pressure p_0	101.3 kPa
Speed of sound in a pure liquid a_ℓ	1483 m/s
Density in a pure liquid ρ_ℓ	998.2 kg/m^3
Polytropic constant γ	1.0
Length of sides of a square duct D	20.0 mm
Input pressure field $P_{\mathrm{in}}(t)$	$P_0[1-\cos\omega(t-x/a_\ell)]$
Nondimensional amplitude P_0/p_0 ($\ll 1$)	2.00×10^{-3}
Nondimensional angular frequency ω/ω_0 ($\ll 1$)	2.00×10^{-3}

by the real and imaginary bubbles:

$$P_{\mathrm{tot}}(t) = P_{\mathrm{in}}(t) + \sum_{i,j(l_{i,j}<l)} \rho_\ell R_0^2 \frac{\ddot{R}'(t-r_{i,j}/a_\ell)}{r_{i,j}}. \tag{2.4.4}$$

We theoretically investigated P_{tot} in Section 2.2. In this section, P_{tot} is calculated by numerically solving Eqs. (2.4.3) and (2.4.4) under numerical conditions shown in Table 2.1. The initial undisturbed bubble radius R_0 is 1.00 mm. The single bubble is placed at $B = 50.0$ mm. The ordinary differential equation (2.4.3) is numerically solved by using the 4-th order Runge-Kutta method.

We investigate the phase speed of the total pressure wave; then, compare it with the speed of sound in a liquid volume that contains a single bubble by Eq. (2.4.1). Let us calculate P_{in} and P_{tot} at the observation point. From these numerical results, we find t' that satisfies the equation $P_{\mathrm{in}}(t) = P_{\mathrm{tot}}(t')$. Then, we define the apparent phase speed of the total pressure wave as $a_{\mathrm{s}}(t)$:

$$a_{\mathrm{s}}(t) = \frac{\Delta x}{\Delta x/a_\ell + t' - t}. \tag{2.4.5}$$

If $a_{\mathrm{s}}(t)$ is equivalent to a_ℓ ($t' = t$), the numerical results lead to the following: the single bubble in the duct cannot reduce the phase speed of the total pressure wave.

Figure 2.5(a) shows the time evolution of P_{in} and P_{tot}. We investigate pressure

(a)

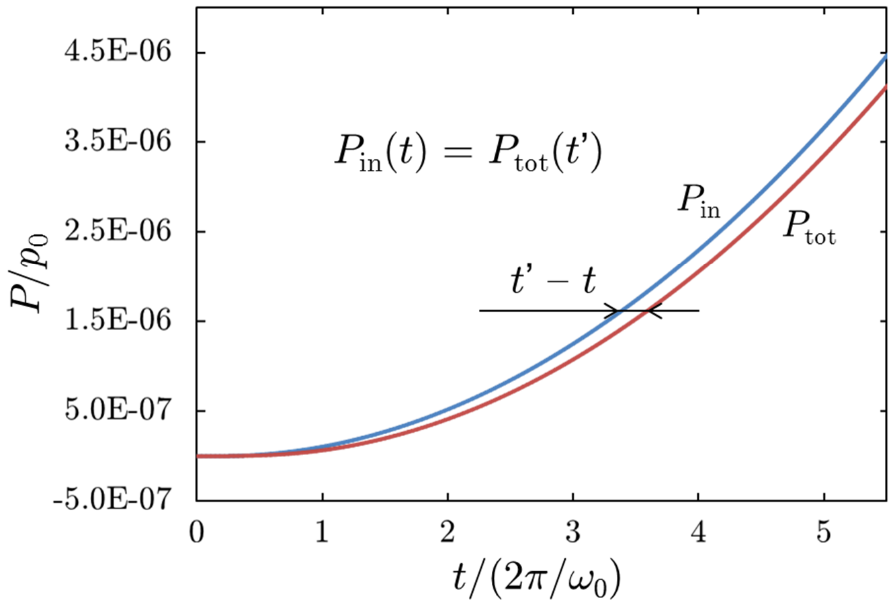

(b)

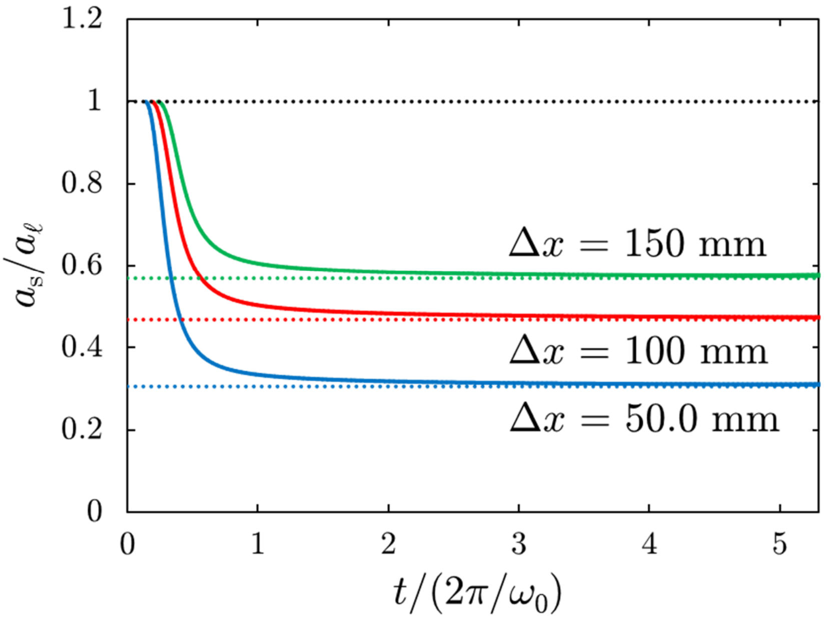

Figure 2.5: (a) Time evolution of P_{in} and P_{tot} in the case of $\Delta x = 100$ mm. (b) Time evolution of the apparent phase speed of the total pressure wave. The black line represents $a_{\mathrm{s}} = a_\ell$.

wave development in the period of the order of $2\pi/\omega_0$, which corresponds to the only 0.1% of the period of the input pressure wave. Figure 2.5(a) clarifies that the single bubble in the duct can indeed delay the phase of the input pressure wave. Figure 2.5(b) shows the time evolution of $a_{\mathrm{s}}(t)$ with various Δx, which is arbitrarily defined. The solid curves in Fig. 2.5(b) represent $a_{\mathrm{s}}(t)$. The dashed lines represent the speed of sound in a liquid volume that contains only a single bubble by Eq. (2.4.1). Figure 2.5(b) clearly shows that the numerically obtained phase speed $a_{\mathrm{s}}(t)$ is apparently reduced from a_ℓ with the lapse of time. Subsequently, $a_{\mathrm{s}}(t)$ approaches to the speed of sound by Eq. (2.4.1).

2.4.2 Discussion

Now, we further consider the refractive index of χ_{s}. We should recall that Δx was arbitrarily defined; since χ_{s} is defined by the use of Eq. (2.4.1), we cannot avoid any arbitrariness in the definition of χ_{s}. In other words, we cannot untangle the dependency between χ_{s} and Δx in a liquid containing only one spherical bubble in a square duct; only the product $(\chi_{\mathrm{s}} - 1)\Delta x$ can be properly defined from Eq. (2.4.1). This failure to uniquely define Δx in Eq. (2.4.1) is equivalent to the failure to uniquely define the void fraction of a liquid containing a single bubble in a square duct, β_{s}. If β_{s} was properly defined, Δx could also be defined; and, χ_{s} could also be defined without ambiguity using Eq. (2.4.1).

Recall that in the definition of χ_{m} in Eq. (2.3.2), we implicitly assumed χ_{m} was a well-defined constant in a volume. In other words, we assumed that the bubbly liquid was a homogeneous continuum medium; therefore, β_{m} was properly defined without ambiguity. However, a volume of liquid containing a single bubble is far from a homogeneous continuum medium; rather, it is a discrete medium for which β_{s} cannot be uniquely defined. Therefore, it is mathematically inadequate to discuss the refractive index of a liquid containing a single bubble, as is understood from Eq. (2.4.1). The refractive index is essentially a value defined only in a properly defined continuum medium.

2.5 Summary

We investigated pressure wave propagation in a square duct filled with a compressible liquid that contains spherical bubbles. We clarified that even a single bubble in a square duct can indeed delay the phase of an input pressure wave, thus causing an apparent reduction in the speed of sound. This is the most fundamental and essential physical process governing pressure wave propagation in a bubbly liquid in a duct.

Next, we discussed the refractive index of a liquid containing a single bubble in a square duct. The refractive index of a liquid containing a single bubble in a square duct cannot be uniquely defined, because the void fraction cannot be uniquely defined. The refractive index is a value defined only within a homogeneous continuum medium; therefore, the refractive index of a liquid containing a single bubble in a square duct itself is neither a physically nor a mathematically meaningful quantity. However, we can observe an apparent reduction in the phase speed in a liquid containing a single bubble in a square duct. Furthermore, we can quantitatively define the speed of sound in a duct containing a finite number of bubbles, when the void fraction can be properly defined.

Chapter 3

Pressure wave propagation in a square duct containing a finite number of bubbles

We theoretically investigated pressure wave propagation in a liquid containing bubbles in a square duct in Chapter 2. We clarified that the apparent reduction in the speed of sound originates from the phase delay of the pressure wave caused by bubble oscillations. These theoretical results imply that the speed of sound in a bubbly liquid can be quantitatively defined in a square duct containing a finite number of bubbles, when the void fraction can be properly defined. However, one critical question is raised; *Can we estimate the speed of sound in a bubbly liquid in a square duct containing several bubbles?*

In this chapter, we numerically investigate pressure wave propagation in a liquid containing 10 spherical bubbles in a square duct. We consider the effect of the pressure fields generated by the surrounding real and imaginary bubbles on the bubble oscillations; hereafter, this effect is collectively called the bubble-bubble interactions. We compare the speed of sound derived in Chapter 2 with the numerically obtained phase speed of the total pressure wave in the duct.

3.1 Problem statement

We numerically investigate pressure wave propagation in a square duct filled with a compressible liquid that contains 10 spherical bubbles (Fig. 3.1). The input plane linear wave $p_0 + P_{\rm in}$ starts to propagate from $x = 0$. The bubbles, which have the same initial undisturbed radius R_0, are evenly aligned along the center-line of the square duct with a separation of Δb. The k-th bubble from the origin is called Bubble k. We perform the simulations under Feynman's regime and the assumptions in Chapter 2 except the assumptions (v) and (vi):

(i). the center of a bubble is fixed in the duct,

(ii). the radial oscillation of a bubble is spherically symmetric,

(iii). a bubble is initially at rest,

(iv). the terms of the attenuation due to the acoustic radiation of order $1/a_\ell$ are neglected,

(v). ~~the number density of bubbles in the~~ $\cancel{y - z}$ ~~plane,~~ $\cancel{\eta}$~~, which is defined as~~ $\cancel{\eta = D^{-2}}$~~, is very close to 0,~~

(vi). ~~the distance between bubbles is sufficiently large so that the bubble-bubble interactions do not appear~~.

Therefore, the radial oscillations of the bubbles are modified by the pressure fields generated by the radial oscillations of the surrounding real and imaginary bubbles.

We shall use the equation of motion for N spherical bubbles [37, 55], where the bubble-bubble interactions are taken into account. Under the present assumptions,

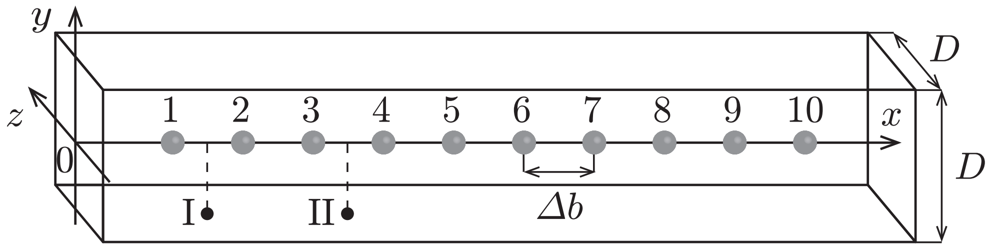

Figure 3.1: 10 spherical bubbles are evenly aligned in a square duct.

the equation of motion for the bubbles can be rewritten as follows:

$$\ddot{R}'_I(t) + \omega_0^2 R'_I(t) = -\frac{P_{\rm in}(t)}{\rho_\ell R_0} - \sum_{J=1,\ J\neq I}^{N} R_0 \frac{\ddot{R}'_J(\zeta_{JI})}{r_{IJ}}, \tag{3.1.1}$$

where the subscripts I and J are the bubble indices $(I, J = 1, 2, \cdots, N, I \neq J)$, r_{IJ} is the distance between the center of the bubble I and the bubble J,

$$\zeta_{JI} = t - \frac{r_{IJ} - R_J(\zeta_{JI})}{a_\ell}, \tag{3.1.2}$$

and $[r_{IJ} - R_J(\zeta_{JI})]/a_\ell$ is the delay time that it takes for the radiative wave generated by the bubble J to propagate the distance r_{IJ} at the speed a_ℓ. In Eq. (3.1.1), we measure the input pressure field $P_{\rm in}(t)$ at the center of the bubble I. The second term in the right-hand side of Eq. (3.1.1) represents the summation of the pressure fields generated by the surrounding bubbles (i.e., the bubble-bubble interactions). In the limit as $r_{IJ} \to \infty$ or $N \to 1$, Eq. (3.1.1) is reduced to the equation of radial motion for a single spherical bubble:

$$\ddot{R}'(t) + \omega_0^2 R'(t) = -\frac{P_{\rm in}(t)}{\rho_\ell R_0}. \tag{2.1.2}$$

The radiative waves generated by the bubbles are reflected off the rigid walls of the duct. We calculate the reflected waves by using the method of images. For each real bubble, we place an infinite number of its imaginary bubbles, as shown

Fig. 2.1(b). Unlike Chapter 2, the bubble oscillations are modified by the pressure fields generated by these imaginary bubbles. The contributions from imaginary bubbles to the bubble oscillations are calculated by using the second term in the right-hand side of Eq. (3.1.1). During a finite time t, the pressure wave propagates only a distance $a_\ell t$; therefore, we need to calculate the pressure fields generated by only the imaginary bubbles within the distance $a_\ell t$ from the bubbles at most.

Now, we calculate the total pressure field at point Q(x, y, z). The total pressure field $P_{\rm tot}$ is given as the summation of $P_{\rm in}(t - x/a_\ell)$ and the pressure fields generated by the radial oscillations of the real and imaginary bubbles. We calculate the pressure field only at finite x and t; therefore, we need to add the contributions from Bubble I and its imaginary bubbles within a circle of radius l_I from point (x_I, y, z) in the $y - z$ plane, where $l_I^2 = (a_\ell t - x_I)^2 - (x - x_I)^2$ and x_I is the x coordinate of the center of Bubble I. The total pressure field $P_{\rm tot}$ can be calculated by using the following equation:

$$P_{\rm tot}(t) = P_{\rm in}(t - x/a_\ell) + \sum_{I=1}^{10} \sum_{i,j(l_{Ii,j}<l_I)} \rho_\ell R_0^2 \frac{\ddot{R}'_I(\zeta_{Ii,j})}{r_{Ii,j}}, \qquad (3.1.3)$$

where $l_{Ii,j}$ is the distance from the point (x_I, y, z) to the center of Bubble $I(i, j)$, $r_{Ii,j}$ is the distance from the center of Bubble $I(i, j)$ to the point Q, and

$$\zeta_{Ii,j} = t - \frac{x_I}{a_\ell} - \frac{r_{Ii,j} - R_I(\zeta_{Ii,j})}{a_\ell}. \qquad (3.1.4)$$

The total pressure field is calculated by numerically solving Eqs. (3.1.1) and (3.1.3) under the numerical conditions in Table 2.1. Bubble 1 is placed at $x = \Delta b$. The distance Δb is 50.0 mm. The ordinary differential equations (3.1.1) are solved numerically by using the 4-th order Runge-Kutta method.

3.2 Numerical results

We investigate the phase speed of the total pressure wave; then, compare it with the speed of sound in a bubbly liquid. Let $P_{\mathrm{I}}(t)$ and $P_{\mathrm{II}}(t)$ be the total pressure fields at points I and II in Fig. 3.1 (at $x = 1.5\Delta b$ and $3.5\Delta b$ on the rigid wall), respectively. From the simulation results, we find t' that satisfies the equation $P_{\mathrm{I}}(t) = P_{\mathrm{II}}(t')$. Then, we define the phase speed as follows:

$$a_{\mathrm{p}}(t) = \frac{2\Delta b}{t' - t}. \tag{3.2.1}$$

We formally define the void fraction in the duct by Eq. (2.3.3), as shown in Chapter 2. We investigate how the phase speed $a_{\mathrm{p}}(t)$ depends on the void fraction β_{m} by changing R_0: 0.550 mm $\leq R_0 \leq 1.00$ mm. The time is normalized by the natural period of the single bubble whose R_0 is 1.00 mm: $2\pi/\omega_0 = 3.60 \times 10^{-4}$ s.

Figure 3.2(a) shows the time evolution of P_{in} at the points I and II. We investigate pressure wave development in the period of the order of $2\pi/\omega_0$, which corresponds to the only 0.1% of the period of the input pressure wave. Figure 3.2(b) shows the time evolution of P_{I} and P_{II} in the case of $R_0 = 1.00$ mm ($R_0/D = 0.05$, $R_0/\Delta b = 0.02$). Figure 3.3(a) shows the time evolution of the phase speeds with various void fractions. The phase speed is reduced from the speed of sound in a pure liquid with the lapse of time. Because the number of contributory imaginary bubbles increases in proportion to t^2, the reliability of the calculation decreases by the accumulation of the error caused by the second term in the right-hand side of Eq. (3.1.1) in the long-time calculation. In the accuracy of the present calculation, we consider that the present solution reaches the steady solution. Therefore, the phase speed of the total pressure wave is reduced in a square duct containing 10 bubbles. We define this steady solution as $\tilde{a}_{\mathrm{p}}$.

(a)

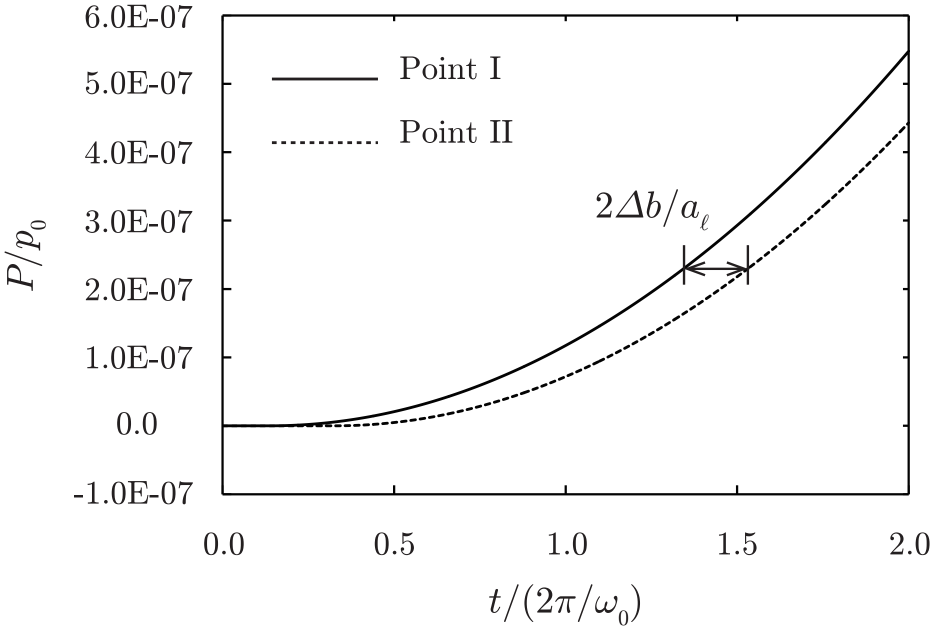

(b)

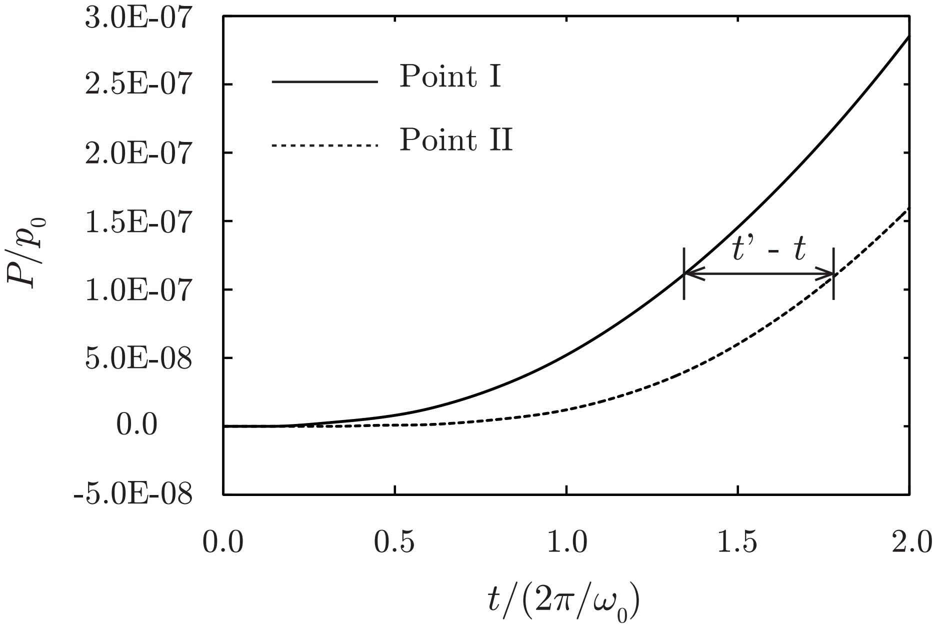

Figure 3.2: (a) Time evolution of P_{in} at the points I and II (ω = 34.9 rad/s). (b) Time evolution of P_{I} and P_{II} in the case of $R_0 = 1.00$ mm.

(a)

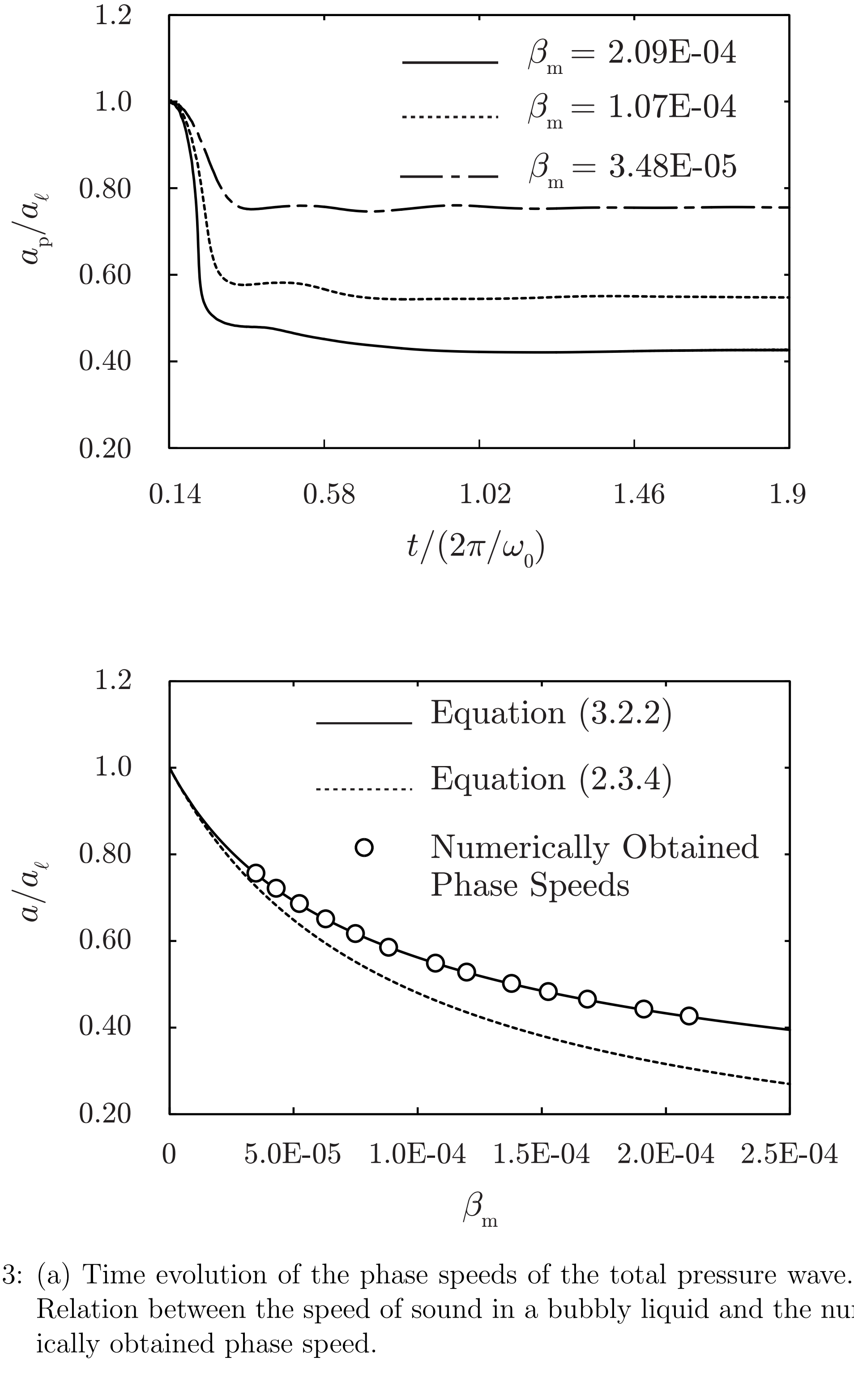

(b)

Figure 3.3: (a) Time evolution of the phase speeds of the total pressure wave. (b) Relation between the speed of sound in a bubbly liquid and the numerically obtained phase speed.

Now, we investigate the phase speed $\tilde{a}_{\rm p}$. We define $\tilde{a}_{\rm p}$ as the phase speed in a time when the input pressure wave reaches the center of Bubble 10, $t = 10\Delta b/a_\ell$ (non-dimensional time: 0.936). Figure 3.3(b) shows the relation between the speed of sound in a bubbly liquid and the numerically obtained phase speed $\tilde{a}_{\rm p}$. The broken curve represents the speed of sound by Eq. (2.3.4). The solid curve represents the speed of sound by

$$a_{\rm m} = a_\ell \left(1 + \frac{\rho_\ell a_\ell^2}{p_0}\beta\right)^{-1/2}. \tag{3.2.2}$$

Equation (3.2.2) is derived from Eq. (1.2.1) when the relation $a_{\rm g}^2 = p_0/\rho_{\rm g}$ is used and the conditions $\beta^2 \ll (\rho_{\rm g} a_{\rm g}^2)/(\rho_\ell a_\ell^2) \ll 1$ are imposed in Eq. (1.2.1). Equation (3.2.2) is identical to Eq. (2.3.4) when the condition $\beta \ll p_0/(\rho_\ell a_\ell^2)$ is imposed. Figure 3.3(b) shows that the phase speed $\tilde{a}_{\rm p}$ agrees well with the speed of sound by Eq. (3.2.2); therefore, the phase speed of the total pressure wave approaches to the speed of sound in a bubbly liquid with the lapse of time.

3.3 Effect of bubble-bubble interactions

Figure 3.3(b) shows that the speed of sound by Eq. (2.3.4) is much lower than the phase speed $\tilde{a}_{\rm p}$ in the high void fraction. To investigate the origin of the difference between the speed of sound by Eq. (2.3.4) and the phase speed $\tilde{a}_{\rm p}$, we will discuss the role of the bubble-bubble interactions in the reduction in the speed of sound in a bubbly liquid. The inclusion of the bubble-bubble interactions means that the input pressure field to induce bubble oscillations is modified by the pressure fields generated by the radial oscillation of bubbles. Figure 3.4 shows the time evolution of R_2. For comparison, we show the numerical result by using the equation without

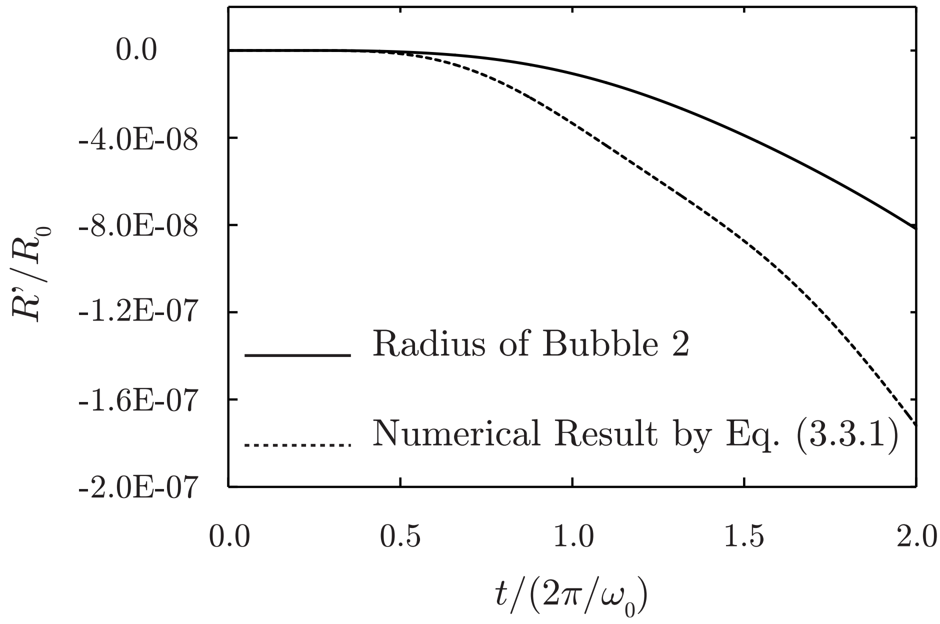

Figure 3.4: Time evolution of R_2 ($R_0 = 1.00$ mm).

the bubble-bubble interactions:

$$\ddot{R}_2'(t) + \omega_0^2 R_2'(t) = -\frac{P_0[1-\cos\omega(t - x_2/a_\ell)]}{\rho_\ell R_0}. \tag{3.3.1}$$

The real and imaginary bubbles are shrunk by the pressure fluctuation induced by the input pressure wave (the compression wave). The shrinking bubbles generate expansion waves. Subsequently, the input pressure field $P_{\rm in}$ to induce the shrinkage of bubbles is attenuated by these expansion waves; therefore, the bubble-bubble interactions suppress the bubble oscillations. For this reason, the shrinkage of Bubble 2 is suppressed by the bubble-bubble interactions, as shown in Fig. 3.4.

The suppression of the bubble oscillations is equivalent to the reduction in the amplitude of the bubble oscillations, s_0. The reduction in s_0 implies the suppression of the phase delay caused by the bubble oscillations, $\Delta\theta = \omega\left(2\pi a_\ell \rho R_0^2 \eta / P_0\right) s_0$, as understood from Eqs. (2.2.1) and (2.2.7); therefore, the bubble-bubble interactions suppress the phase delay $\Delta\theta$. The apparent reduction in the speed of sound in a bubbly liquid originates from the phase delay $\Delta\theta$, as understood from Chapter 2. The suppression of the phase delay $\Delta\theta$ implies the suppression of the apparent reduction in the speed of sound; therefore, the bubble-bubble interactions suppress the reduction in the phase speed of the total pressure field. For this reason, the speed of sound by Eq. (2.3.4), where the bubble-bubble interactions are neglected, is lower than $\tilde{a}_{\mathrm{p}}$, where the bubble-bubble interactions are taken into account, in the high void fraction, where the bubble-bubble interaction can no longer be ignored. We conclude that the bubble-bubble interactions suppress the apparent reduction in the speed of sound in a bubbly liquid.

3.4 Effect of delay times

The acoustic radiation and the delay time are taken into account in the equation of motion for the bubbles in a compressible liquid. In this study, all attenuations, including the acoustic radiation of order $1/a_\ell$, are ignored; however, the delay time is considered (where the delay time is defined as the finite amount of time that it takes for a pressure wave to propagate a given distance with the speed of sound in a pure liquid). Equations (3.1.2) and (3.1.4) contain the delay times.

Now, we will discuss the role of the delay times in the summation of the pressure fields. We have investigated bubble oscillations in a square duct. The radiative waves generated by bubbles are reflected off the rigid walls of the duct. We determine the reflected waves by calculating the pressure fields due to the oscillations of imaginary bubbles placed into a two-dimensional array in the $y-z$ plane, as shown Fig. 2.1(b). We calculate the total pressure field by adding all the pressure fields which can reach observation points during a finite time t (Fig. 3.5). Because the wave propagation distance increases with the lapse of time, we need to consider the pressure fields

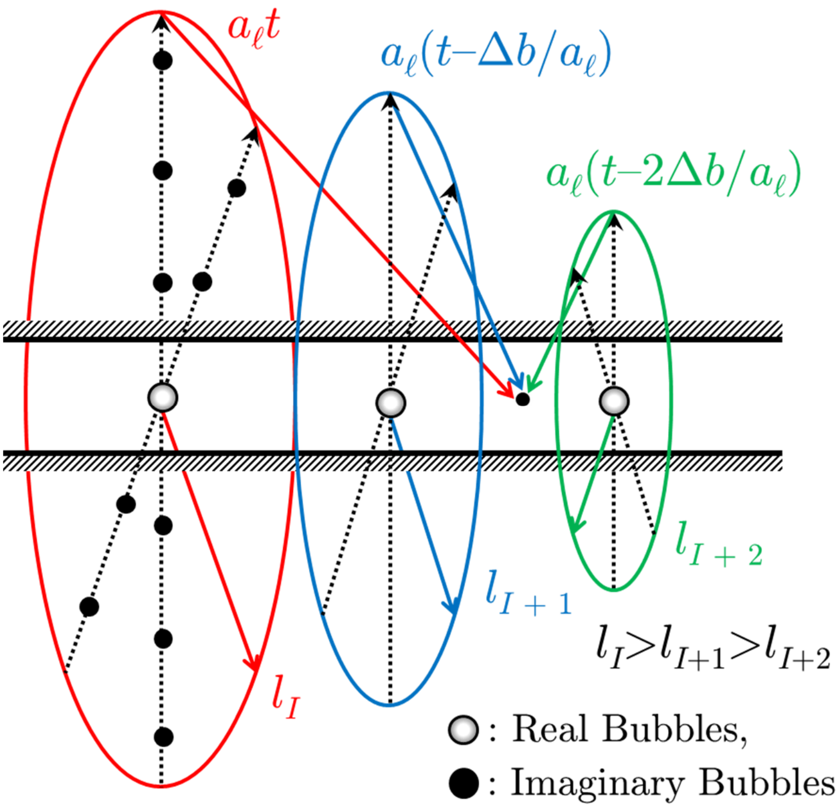

Figure 3.5: The total pressure field is calculated by adding the pressure fields generated by bubbles within a circle of radius l_I in each layer. The radius l_I is different in accordance with positions of the layers because the starting time of bubble oscillations in each layer is different. The distance between adjacent layers is Δb; therefore, the difference of the starting time of bubble oscillations is $\Delta b/a_\ell$.

generated by the farther bubbles. The delay times are different in accordance with the distance between the bubbles and observation points; therefore, the phases of these pressure fields deviate from each other depending on the path difference.

In this chapter, we have investigated pressure wave propagation in a square duct containing 10 spherical bubbles by numerically solving Eqs. (3.1.1) and (3.1.3) which take the bubble-bubble interactions into account. We have calculated the total pressure field by adding the pressure fields generated by radial oscillation of individual bubbles, where the phase shifts caused by the delay times are considered. When the distance between bubbles and observation points becomes far, the amplitudes of the pressure fields generated by the bubble oscillations decrease; then, the phase shifts of these pressure fields increase. The summation of these pressure fields converges with the lapse of time, as understood from Section 2.2; however, the orbit of the summation of the pressure fields until the convergence is different from that shown in Fig. 2.2(b) because we have investigated pressure wave propagation in a square duct containing several bubbles in this chapter. In Chapter 2, we theoretically investigated the total pressure field after the lapse of the time that is enough for P_{bs} to converge. In contrast, we have numerically investigated the time evolution of the summation of the pressure fields in this chapter. While the summation of the pressure fields converges with the lapse of time, the phase speed in the total pressure wave changes from the speed of sound in a pure liquid to that in a bubbly liquid.

If the delay times are ignored ($a_\ell \to \infty$, i.e., the liquid phase is assumed to be incompressible), the pressure fields generated by an infinite number of imaginary bubbles immediately contribute to the total pressure field with the same phase. The summation of these pressure fields immediately amounts to a very large and non-physical value without converging. Therefore, the summation of the pressure fields in Eqs. (2.2.1) and (3.1.3) cannot have a physically appropriate value without taking into account the phase shifts caused by the delay times. The phase shifts caused by the delay times converge the summation of the pressure fields to a physically appropriate value.

3.5 Effect of the number of bubbles

Now, we will investigate a relation between the phase speed of the total pressure wave and the number of bubbles evenly aligned in a square duct. We numerically calculate the time evolution of the phase speed defined by Eq. (3.2.1) while we reduce the number of bubbles aligned in the duct one by one in descending order.

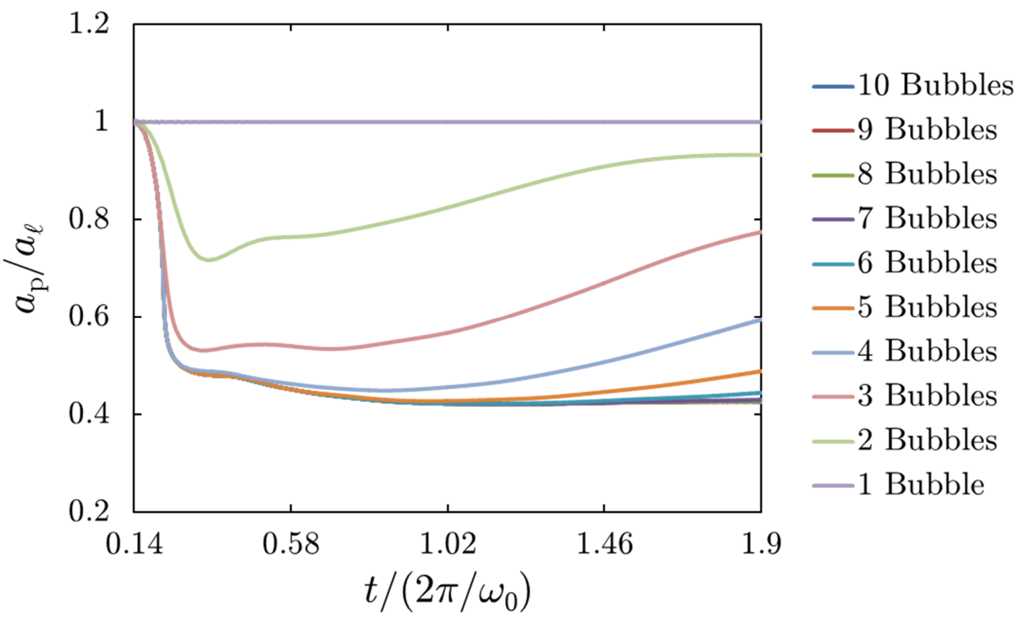

Figure 3.6: Time evolution of the phase speeds with various number of bubbles.

Figure 3.6 shows the time evolution of the phase speeds with various number of bubbles. Figure 3.6 shows that the phase speed is reduced even if we reduce the number of bubbles in the downstream region of the point II; however, when only a few bubbles are aligned in the downstream region of the point II, the phase speed deviates from the speed of sound in a bubbly liquid with the lapse of time.

The time evolution of the phase speed is drastically varied by the removal of all the bubbles in the downstream region of the point II (the cases of "3 Bubbles" and "2 Bubbles"). Furthermore, when we remove all the bubbles in the downstream region of the points I and II (a single bubble is placed in the upstream region of the point I, i.e., the case of "1 Bubble"), the phase speed is not reduced, despite the presence of bubble in the upstream region of the point I. Therefore, the pressure fields generated by bubbles in the downstream region of observation points cause the reduction in the phase speed of the total pressure wave; however, the pressure fields generated by bubbles in the upstream region of observation points cannot contribute to the reduction in the phase speed defined by Eq. (3.2.1).

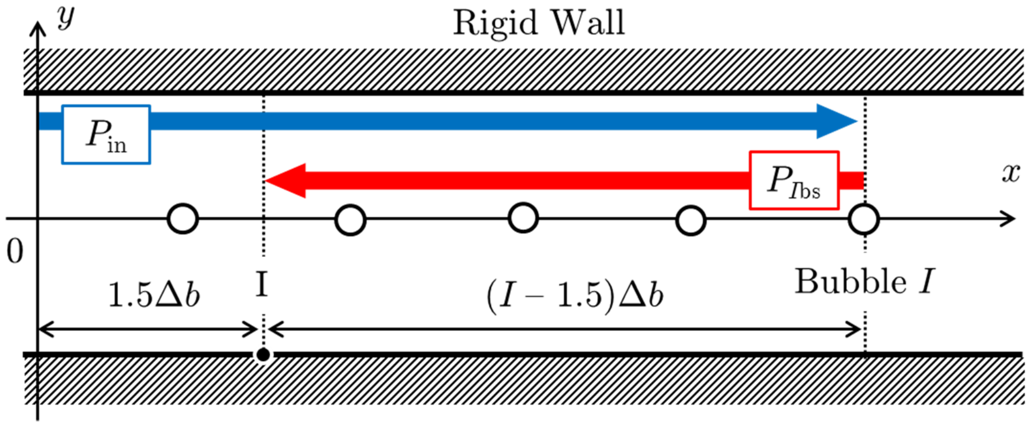

Figure 3.7: The input pressure field P_{in} induces the radial oscillation of Bubble I. Subsequently, the pressure field $P_{I\mathrm{bs}}$ is generated, and propagates in the negative x direction.

Let us consider that k bubbles evenly aligned in the duct are shrunk by the input pressure wave ($1 < k \leq 10$). We define the summation of the pressure fields generated by Bubble I and its imaginary bubbles in the downstream region of the point I as $P_{I\mathrm{bs}}$ ($I > 1$). The arrival time t_I, which is the time that it takes for $P_{I\mathrm{bs}}$ to reach the point I, can be roughly written as follows (Fig. 3.7):

$$t_I = \frac{I\Delta b + (I - 1.5)\Delta b}{a_\ell}. \tag{3.5.1}$$

When $t < t_{k+1}$, the pressure fields generated by bubbles placed in the downstream region of the k bubbles never reach the point I within the observation time t; therefore, these pressure fields never contribute to the total pressure field at the point I. In the case of "10 Bubbles", the present observation time, $t/(2\pi/\omega_0) = 1.90$, satisfies the equation $t < t_{11}$ because $t_{11}/(2\pi/\omega_0) = 1.92$. Therefore, even if bubbles are evenly aligned in the downstream region of Bubble 10, the pressure fields generated by these bubbles never contribute to the total pressure field at the point I within the present observation time.

When we remove the bubbles in the downstream region of the point I ($k < 10$), the pressure fields generated by these bubbles, which should originally reach the point I, disappear; then, $t_{k+1} < t$. Figure 3.6 shows that when t_{k+1} is much shorter than the present observation time, the phase speed deviates from the speed of sound in a bubbly liquid.

In a square duct containing 10 bubbles, Fig. 3.3(a) shows that the phase speed of the total pressure wave reaches a constant value, which agrees well with the speed of sound by Eq. (3.2.2). However, when t is much longer than t_{k+1}, the phase speed will deviate from the constant value with the lapse of time, even though we perform the simulations in a square duct containing *10 bubbles*. Therefore, we conclude that the number of bubbles itself is not necessarily important in the reduction in the phase speed of the total pressure wave in a square duct.

3.6 Summary

We numerically investigated pressure wave propagation in a square duct containing a finite number of bubbles. We simulated linear plane wave propagation in a liquid containing 10 spherical bubbles in the duct by using the equation of motion for N spherical bubbles, where the effect of the bubble-bubble interactions is taken into account. The numerical results show that the phase speed of the total pressure wave is reduced from the speed of sound in a pure liquid to that in a bubbly liquid.

Furthermore, we investigated the effect of the bubble-bubble interactions on the speed of sound. We clarified that the bubble-bubble interactions suppress the reduction in the speed of sound in a bubbly liquid.

Next, we discussed the effect of the delay times on the summation of the pressure fields. The phase shifts caused by the delay times converge the summation of the pressure fields to a physically appropriate value.

Finally, we numerically investigated a relation between the phase speed of the total pressure wave and the number of bubbles aligned in a square duct. The pressure fields generated by bubbles in the downstream region of observation points cause the reduction in the phase speed of the total pressure wave; however, the pressure fields generated by bubbles in the upstream region of observation points cannot contribute to the reduction in the phase speed. We conclude that the number of bubbles itself is not necessarily important in the reduction in the phase speed in a square duct.

Chapter 4

Phase speed in a square duct containing a single bubble

We numerically investigated pressure wave propagation in a square duct containing a finite number of bubbles in Chapter 3. The numerical results showed that even if only 10 bubbles are aligned in the duct, the phase speed of the total pressure wave is reduced from the speed of sound in a pure liquid to that in a bubbly liquid. Furthermore, we clarified that the number of bubbles itself is not necessarily important in the reduction in the phase speed in a square duct.

In this chapter, we theoretically investigate the phase speed of the total pressure wave in a square duct containing *just one bubble.* We construct the theoretical model for the radial oscillation of a single bubble affected by the pressure waves reflected off the rigid walls of the duct. We will clarify how these reflected waves modify the bubble oscillation and the total pressure field in the duct. Furthermore, we investigate the phase speed of the total pressure wave in the duct based on the theoretical model. It should be emphasized here that in this study inspired by Feynman *et al.* [85], <u>the phase speed of the total pressure wave is the speed of sound in a bubbly liquid.</u>

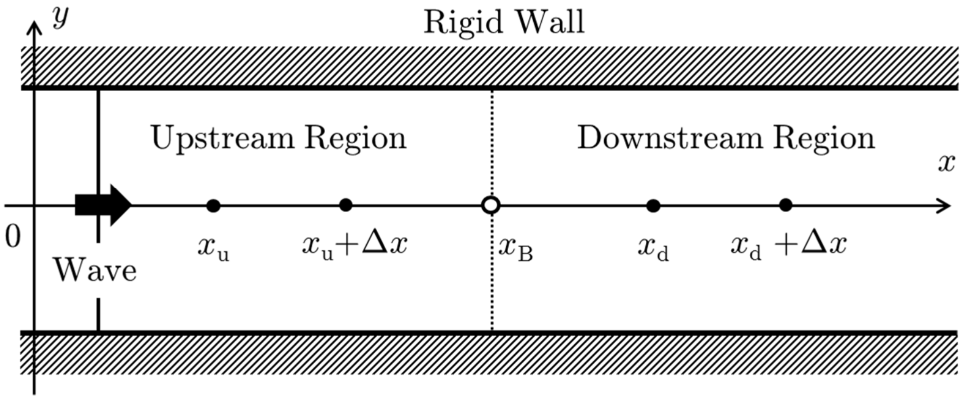

Figure 4.1: Schematic of the $x-y$ plane of the computational domain.

4.1 Radial oscillation of a single bubble affected by reflected waves

We theoretically investigate pressure wave propagation in a square duct with sides of length D filled with a compressible liquid that contains a single bubble placed at x_{B} (Fig. 4.1). The input plane linear wave starts to propagate from $x=0$. The input plane wave has the following form: $p_0 + P_{\mathrm{in}}(t) = p_0 + P_0 \mathrm{e}^{\mathrm{i}\omega t}$.

Now, we investigate the radial oscillation of a spherical bubble in a square duct under the assumptions in Chapter 3. We determine the pressure waves reflected off the rigid walls of the duct by using the method of images, as shown in Fig. 2.1(b). The radial oscillation of the real bubble is modified by the pressure fields generated by the surrounding imaginary bubbles. We can calculate the radial oscillation of the single bubble in the duct by using the following equation:

$$\ddot{R}'(t) + \omega_0^2 R'(t) = -\frac{P_{\mathrm{in}}(t)}{\rho_\ell R_0} - \sum_{i,j(l_{i,j}<a_\ell t)} R_0 \frac{\ddot{R}'_{\mathrm{im}}(t - l_{i,j}/a_\ell)}{l_{i,j}}, \tag{4.1.1}$$

where $R'_{\mathrm{im}}(t)$ is the small fluctuation of the imaginary bubble radius: $R'_{\mathrm{im}}(t) = R_{\mathrm{im}}(t) - R_0$. In Chapter 2, $R'_{\mathrm{im}}(t) = R'(t)$. The second term in the right-hand side of Eq. (4.1.1) represents the effect of the summation of the pressure fields generated by the imaginary bubbles on the real bubble oscillation, which is defined as $P_{\rm ims}/(\rho_\ell R_0)$. The pressure field $P_{\rm ims}$ is equivalent to the summation of the reflected waves that affect the real bubble oscillation. Strictly speaking, the radial oscillations of the imaginary bubbles should be modified depending on the modified real bubble oscillation. However, we impose the following assumption:

(vii). the pressure fields generated by the imaginary bubbles affect the real bubble oscillation, but the influence of the modified real bubble oscillation on the imaginary bubbles is neglected.

In this assumption, we take advantage that $R'_{\rm im}(t)$ always satisfies the following linear equation:

$$\ddot{R}'_{\rm im}(t) + \omega_0^2 R'_{\rm im}(t) = -\frac{P_{\rm in}(t)}{\rho_\ell R_0}. \tag{4.1.2}$$

By solving Eq. (4.1.2), we can write $R'_{\rm im}(t)$ as a function of time: $R'_{\rm im}(t) = -s_0 {\rm e}^{{\rm i}\omega t}$. Therefore, we can calculate $P_{\rm ims}(t)/(\rho_\ell R_0)$ as follows:

$$\frac{P_{\rm ims}(t)}{\rho_\ell R_0} = -\sum_{i,j(l_{i,j}<a_\ell t)} R_0 \frac{\omega^2 s_0 {\rm e}^{{\rm i}\omega(t-l_{i,j}/a_\ell)}}{l_{i,j}} = {\rm i}\Delta\theta \frac{P_0}{\rho_\ell R_0} {\rm e}^{{\rm i}\omega t}. \tag{4.1.3}$$

We follow the same procedure as Chapter 2 in performing the summation in Eq. (4.1.3). We suppose that this procedure on the calculation of the total pressure field can also be established at the point B (the bubble center) in Fig. 2.1(a). By substituting $P_{\rm ims}(t)/(\rho_\ell R_0)$ into Eq. (4.1.1), we can solve Eq. (4.1.1) as follows:

$$R(t) = R_0 - (1 - {\rm i}\Delta\theta) s_0 {\rm e}^{{\rm i}\omega t} \simeq R_0 - s_0 {\rm e}^{{\rm i}\omega(t-\Delta\theta/\omega)}. \tag{4.1.4}$$

When we ignore the effect of the pressure fields generated by the imaginary bubbles (the reflected waves) on the real bubble oscillation, $R(t)$ is written by

$$R(t) = R_0 - s_0 \mathrm{e}^{\mathrm{i}\omega t},$$

as understood from Section 2.1. Equation (4.1.4) clarifies that the reflected waves retard the phase of the bubble oscillation by the angle $\Delta\theta/\omega$.

We investigate the total pressure field at point Q$(x, 0, 0)$. The summation of the pressure fields generated by the real and imaginary bubbles , P_{bs}, can be written by

$$P_{\mathrm{bs}}(t) = \rho_\ell R_0^2 \frac{\ddot{R}'(t - \Delta\theta/\omega - r/a_\ell)}{r} + \sum_{i,j(l_{i,j}<l)} \rho_\ell R_0^2 \frac{\ddot{R}'_{\mathrm{im}}(t - r_{i,j}/a_\ell)}{r_{i,j}}, \tag{4.1.5}$$

where $r = |x - x_{\mathrm{B}}|$ and $r_{i,j}^2 = r^2 + l_{i,j}^2$. We replace $R'_{\mathrm{im}}(t)$ with $R'(t)$ which is obtained from Eq. (4.1.4); then, we can calculate P_{bs} as follows:

$$\begin{aligned} P_{\mathrm{bs}}(t) &= \sum_{i,j(l_{i,j}<l)} \rho_\ell R_0^2 \frac{\omega^2 s_0 \exp[\mathrm{i}\omega(t - \Delta\theta/\omega - r_{i,j}/a_\ell)]}{r_{i,j}} \\ &= -\mathrm{i}\Delta\theta P_0 \exp\left[\mathrm{i}\omega\left(t - \frac{\Delta\theta}{\omega} - \frac{|x - x_{\mathrm{B}}|}{a_\ell}\right)\right]. \end{aligned} \tag{4.1.6}$$

Therefore, the total pressure field at the point Q is given by

$$P_{\mathrm{tot}}(t) = P_0 \exp\left[\mathrm{i}\omega\left(t - \frac{x}{a_\ell}\right)\right] - \mathrm{i}\Delta\theta P_0 \exp\left[\mathrm{i}\omega\left(t - \frac{\Delta\theta}{\omega} - \frac{x_{\mathrm{B}} + |x - x_{\mathrm{B}}|}{a_\ell}\right)\right]. \tag{4.1.7}$$

When we ignore the effect of the reflected waves on the real bubble oscillation, $P_{\mathrm{tot}}(t)$ is written by

$$P_{\mathrm{tot}}(t) = P_0 \exp\left[\mathrm{i}\omega\left(t - \frac{x}{a_\ell}\right)\right] - \mathrm{i}\Delta\theta P_0 \exp\left[\mathrm{i}\omega\left(t - \frac{x_{\mathrm{B}} + |x - x_{\mathrm{B}}|}{a_\ell}\right)\right],$$

as understood from Section 2.2. Equation (4.1.7) clarifies that the pressure fields generated by the imaginary bubbles retard the phase of P_{bs} generated by themselves by the angle $\Delta\theta/\omega$.

4.2 Variation of the phase speed around a single bubble

When bubbles are not placed in a square duct, the phase speed of the total pressure wave is the speed of sound in a pure liquid. We theoretically investigate the variation of the phase speed in a square duct containing a single bubble. We investigate the phase speed in both a downstream region and an upstream region, as shown in Fig. 4.1. In this section, we suppose that $P_{\mathrm{in}}(t) = P_0 \cos\omega t$.

4.2.1 Downstream region

First, we investigate the phase speed in the downstream region. Let P_{d} and $P_{\mathrm{d}+\Delta x}$ be the total pressure fields at points x_{d} and $x_{\mathrm{d}} + \Delta x$ in Fig. 4.1, respectively. We consider t' that satisfies the equation $P_{\mathrm{d}}(t) = P_{\mathrm{d}+\Delta x}(t')$ by using Eq. (4.1.7) as follows:

$$\begin{aligned} &\cos\omega\left(t - \frac{x_{\mathrm{d}}}{a_\ell}\right) + \Delta\theta \sin\omega\left(t - \frac{\Delta\theta}{\omega} - \frac{x_{\mathrm{d}}}{a_\ell}\right) \\ &= \cos\omega\left(t' - \frac{x_{\mathrm{d}} + \Delta x}{a_\ell}\right) + \Delta\theta \sin\omega\left(t' - \frac{\Delta\theta}{\omega} - \frac{x_{\mathrm{d}} + \Delta x}{a_\ell}\right). \end{aligned} \tag{4.2.1}$$

From the phase functions of Eq. (4.2.1), we obtain the following equation: $t' = t + \Delta x / a_\ell$. We define the phase speed of the total pressure wave:

$$v_{\mathrm{p}}(t) = \frac{\Delta x}{t' - t}. \tag{4.2.2}$$

Then, we obtain the phase speed in the downstream region, $v_{\mathrm{p}}(t) = a_\ell$. Therefore, in the downstream region, the phase speed of the total pressure wave is not varied from the speed of sound in a pure liquid. This result had been numerically validated in Section 3.5. As we had stated in Section 3.5, the pressure fields generated by bubbles in the upstream region of observation points cannot contribute to the reduction in the phase speed.

4.2.2 Upstream region

Next, we investigate the phase speed in the upstream region. Let P_{u} and $P_{\mathrm{u}+\Delta x}$ be the total pressure fields at points x_{u} and $x_{\mathrm{u}} + \Delta x$ in Fig. 4.1, respectively. We consider t' that satisfies the equation $P_{\mathrm{u}}(t) = P_{\mathrm{u}+\Delta x}(t')$ by using Eq. (4.1.7) as follows:

$$\begin{aligned}
&\cos\omega\left(t - \frac{x_{\mathrm{u}}}{a_\ell}\right) + \Delta\theta \sin\omega\left(t - \frac{\Delta\theta}{\omega} - \frac{x_{\mathrm{B}} + x_{\mathrm{B}} - x_{\mathrm{u}}}{a_\ell}\right) \\
&= \cos\omega\left(t' - \frac{x_{\mathrm{u}} + \Delta x}{a_\ell}\right) + \Delta\theta \sin\omega\left[t' - \frac{\Delta\theta}{\omega} - \frac{x_{\mathrm{B}} + x_{\mathrm{B}} - (x_{\mathrm{u}} + \Delta x)}{a_\ell}\right]. \qquad (4.2.3)
\end{aligned}$$

From Eq. (4.2.3), we obtain the following equation:

$$\sin\left[\omega\Delta t + \alpha(t)\right] = \frac{1}{\psi}\left[-\cos\omega\left(\frac{\Delta x}{a_\ell} + \nu\right) + \Delta\theta\sin\omega\left(\frac{\Delta x}{a_\ell} - \xi\right)\right] = \Gamma(t), \qquad (4.2.4)$$

with

$$\begin{aligned}
&\nu = t - \frac{x_{\mathrm{u}} + \Delta x}{a_\ell}, \quad \xi = t - \frac{\Delta\theta}{\omega} - \frac{x_{\mathrm{B}} + x_{\mathrm{B}} - (x_{\mathrm{u}} + \Delta x)}{a_\ell}, \\
&\psi = \sqrt{1 + 2\Delta\theta\sin\omega(\xi - \nu) + \Delta\theta^2}, \quad \alpha(t) = \arcsin\frac{1}{\psi}\left(-\cos\omega\nu - \Delta\theta\sin\omega\xi\right).
\end{aligned}$$

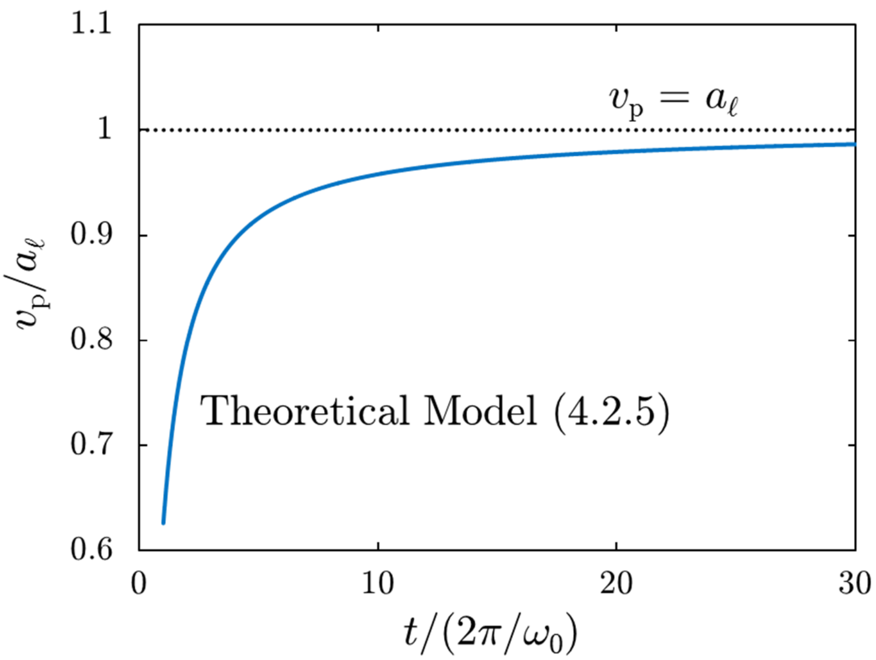

Figure 4.2: Time evolution of the phase speed by Eq.(4.2.5) with $R_0 = 1.00$ mm, $x_{\rm B} = 250$ mm, $x_{\rm u} = 75.0$ mm, $\Delta x = 100$ mm, and the conditions shown in Table 2.1.

From Eq. (4.2.4), the phase speed in the upstream region can be obtained as a function of time:

$$v_{\rm p}(t) = \frac{\omega \Delta x}{\arcsin[\Gamma(t)] - \alpha(t)}, \quad t > \frac{\Delta\theta}{\omega} + \frac{x_{\rm B} + x_{\rm B} - x_{\rm u}}{a_\ell}. \tag{4.2.5}$$

Equation (4.2.5) shows that the phase speed of the total pressure wave is the function of time in the upstream region. Figure 4.2 shows the time evolution of the theoretical model (4.2.5). The solid (blue) curve represents the phase speed by Eq. (4.2.5). The dotted (black) line represents $v_{\rm p} = a_\ell$. Figure 4.2 shows that in the period of the order of the natural period of the bubble, the phase speed by Eq. (4.2.5) in the upstream region is lower than a_ℓ at least.

4.3 Comparison with numerical results

To validate this theoretical model, we numerically investigate the phase speed of the total pressure wave in the upstream region by using Eqs. (2.4.3) and (2.4.4):

$$\ddot{R}'(t) + \omega_0^2 R'(t) = -\frac{P_{\rm in}(t)}{\rho_\ell R_0} - \sum_{i,j(l_{i,j}<a_\ell t)} R_0 \frac{\ddot{R}'(t - l_{i,j}/a_\ell)}{l_{i,j}}, \tag{2.4.3}$$

$$P_{\rm tot}(t) = P_{\rm in}(t) + \sum_{i,j(l_{i,j}<l)} \rho_\ell R_0^2 \frac{\ddot{R}'(t - r_{i,j}/a_\ell)}{r_{i,j}}. \tag{2.4.4}$$

We compare the numerically obtained phase speed with the phase speed by Eq. (4.2.5). We suppose the following conditions: $R_0 = 1.00$ mm, $x_{\rm B} = 250$ mm, $x_{\rm u} = 75.0$ mm, and $\Delta x = 100$ mm. The ordinary differential equation (2.4.3) is numerically solved by using the 4-th order Runge-Kutta method under the conditions in Table 2.1.

Figure 4.3(a) shows the time evolution of $P_{\rm bs}$ at $x_{\rm u}$. The solid (blue) curve in Fig. 4.3(a) represents the numerically obtained $P_{\rm bs}$. The dotted (red) curve represents the theoretical model (4.1.6). Figure 4.3(a) shows that the theoretical model (4.1.6) agrees well with the numerical result obtained from Eqs. (2.4.3) and (2.4.4). Figure 4.3(b) shows the time evolution of $P_{\rm u}$ and $P_{{\rm u}+\Delta x}$. From this numerical result, we find t' that satisfies $P_{\rm u}(t) = P_{{\rm u}+\Delta {\rm x}}(t')$; then, we define the phase speed as follows: $v_{\rm p} = \Delta x/(t' - t)$.

Figure 4.4 shows the time evolution of the phase speed in the upstream region. The solid (blue) curve in Fig. 4.4 represents the numerically obtained phase speed. The broken (red) curve represents the theoretical model (4.2.5). The dotted (black) line represents $v_{\rm p} = a_\ell$. The numerically obtained phase speed is reduced from a_ℓ with the lapse of time. After a certain period of time, the numerically obtained phase speed agrees well with the theoretical model (4.2.5). The phase speed by Eq. (4.2.5) approaches to a_ℓ with the lapse of long time; however, the phase speed does not exceed a_ℓ under the present conditions. Therefore, even if just one bubble is

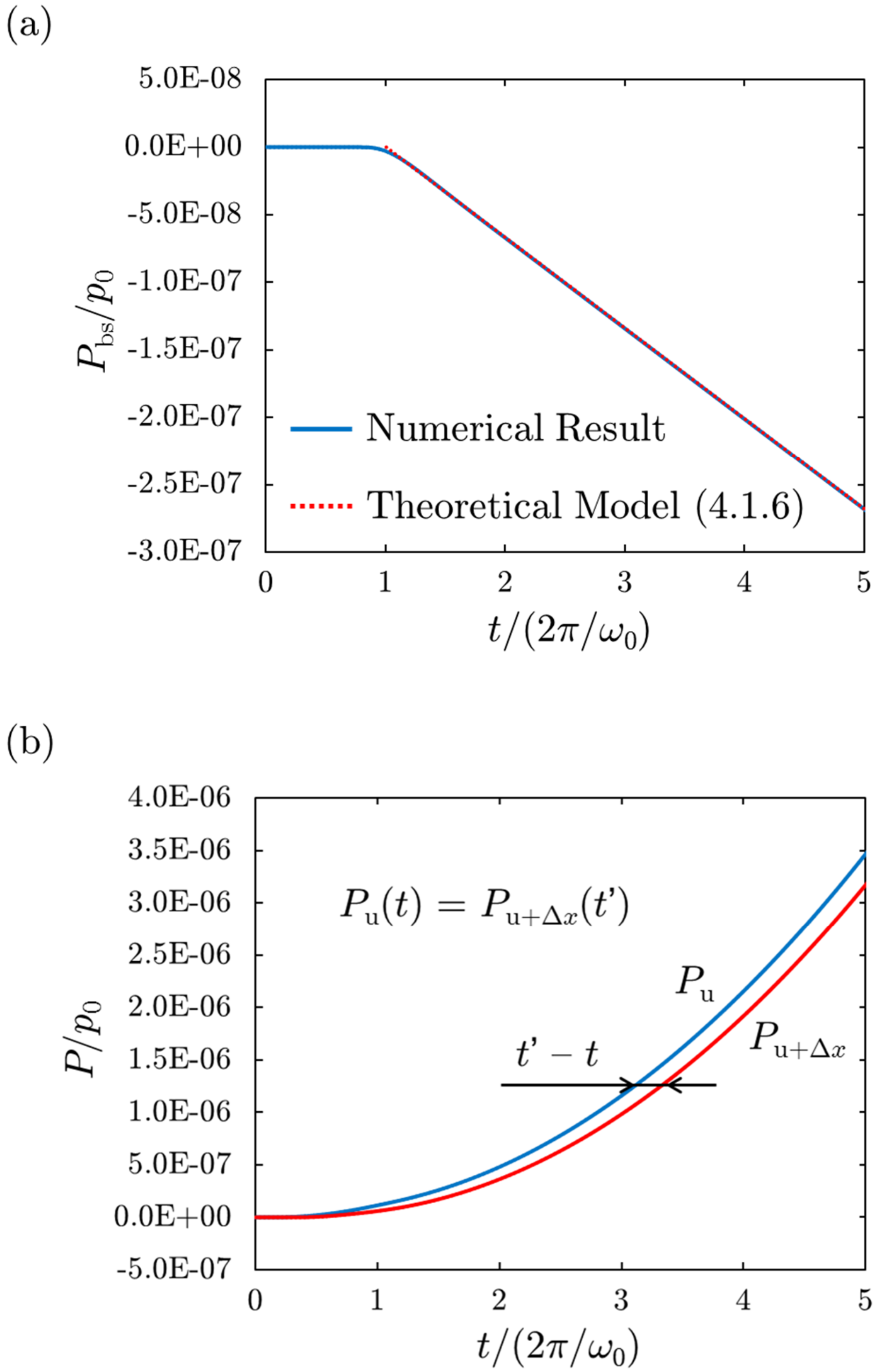

Figure 4.3: (a) Time evolution of P_{bs} at x_{u}. (b) Time evolution of P_{u} and $P_{\mathrm{u}+\Delta x}$.

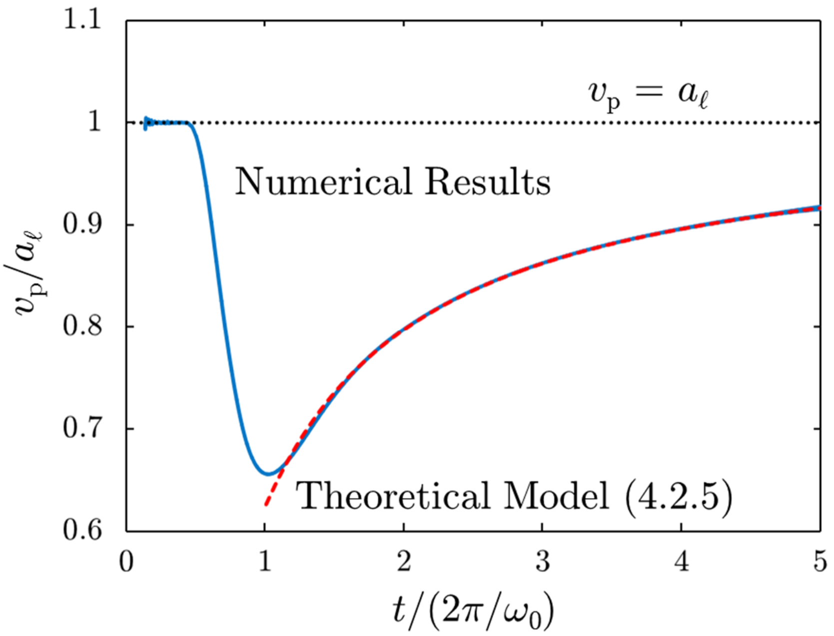

Figure 4.4: Time evolution of the phase speed of the total pressure wave obtained by the numerical calculation and that by the theoretical model in the upstream region.

placed in a square duct, the phase speed of the total pressure wave in the upstream region is lower than a_ℓ at least.

4.4 Summary

We theoretically investigated pressure wave propagation in a square duct containing just one bubble. We constructed the theoretical model for the radial oscillation of a single bubble affected by the reflected waves. This model shows that the reflected waves retard the phase of the bubble oscillation and that of the summation of the pressure fields generated by the real and imaginary bubbles. Based on this model, we constructed the theoretical model for the phase speed of the total pressure wave in a square duct containing just one bubble. The phase speed is not varied from a_ℓ in the downstream region of the bubble. In contrast to the downstream region, the phase speed in the upstream region is the function of time.

To validate our model, we numerically investigated the phase speed in the upstream region. The phase speed in the upstream region is reduced from the speed of sound in a pure liquid with the lapse of time. After a certain period of time, the numerically obtained phase speed agrees well with our model. The theoretical and numerical results clarified that even if just one bubble is placed in the duct, the phase speed in the upstream region is lower than the speed of sound in a pure liquid at least.

Chapter 5

Conclusions

We investigated pressure wave propagation in a square duct containing a finite number of spherical bubbles. The contributions and findings of this thesis can be summarized as follows.

Chapter 2

We theoretically investigated pressure wave propagation in a square duct filled with a compressible liquid that contains spherical bubbles, based on the following Feynman's regime:

- the total pressure field can always be represented by the summation of the pressure fields generated by the input pressure wave and the oscillations of all the bubbles,
- the pressure field generated by a single bubble is given by its oscillation evaluated with retardation at the speed of sound in a pure liquid.

We clarified that even a single bubble in a square duct can indeed delay the phase of an input pressure wave, thus causing an apparent reduction in the speed of sound.

This is the most fundamental and essential physical process governing pressure wave propagation in a bubbly liquid in a duct.

Next, we discussed the refractive index of a liquid containing a single bubble in a square duct. The refractive index of a liquid containing a single bubble in a square duct cannot be uniquely defined, because the void fraction cannot be uniquely defined. However, we can observe an apparent reduction in the phase speed in a liquid containing a single bubble in a square duct.

Chapter 3

We numerically investigated pressure wave propagation in a square duct containing a finite number of bubbles. The numerical results showed that the numerically obtained phase speed of the total pressure wave is reduced from the speed of sound in a pure liquid to that in a bubbly liquid.

Furthermore, we investigated the effect of the bubble-bubble interactions on the speed of sound. We clarified that the bubble-bubble interactions suppress the reduction in the speed of sound in a bubbly liquid.

Next, we discussed the effect of the delay time on the summation of the pressure fields. The phase shifts caused by the delay times converge the summation of the pressure fields to a physically appropriate value.

Finally, we investigated a relation between the phase speed of the total pressure wave and the number of bubbles in a square duct. The pressure fields generated by bubbles in the downstream region of observation points cause the reduction in the phase speed of the total pressure wave; however, the pressure fields generated by bubbles in the upstream region cannot contribute to the reduction in the phase speed. The number of bubbles itself is not necessarily important in the reduction in the phase speed in a square duct.

Chapter 4

We theoretically investigated pressure wave propagation in a square duct containing just one bubble. The reflected waves retard the phase of the bubble oscillation and that of the summation of the pressure fields generated by the real and imaginary bubbles. We constructed the theoretical model for the phase speed of the total pressure wave in a square duct containing just one bubble. In the downstream region of the bubble, the phase speed is not varied from the speed of sound in a pure liquid. In contrast to the downstream region, the phase speed in the upstream region is the function of time.

To validate our model, we numerically investigated the phase speed in the upstream region. The numerically obtained phase speed agrees well with our model. The theoretical and numerical results clarified that even if just one bubble is placed in the duct, the phase speed in the upstream region is lower than the speed of sound in a pure liquid at least.

References

[1] Y. Matsumoto, J. S. Allen, S. Yoshizawa, T. Ikeda, and Y. Kaneko. Medical ultrasound with microbubbles. *Exp. Therm. Fluid Sci.*, Vol. 29, pp. 255–265, 2005.

[2] T. Kodama, Y. Tomita, Y. Watanabe, K. Koshiyama, T. Yano, and S. Fujikawa. Cavitation bubbles mediated molecular delivery during sonoporation. *J. Biomech. Sci. Eng.*, Vol. 4, No. 1, pp. 124–140, 2009.

[3] A. Prosperetti, N. Q. Lu, and H. S. Kim. Active and passive acoustic behavior of bubble clouds at the ocean's surface. *J. Acoust. Soc. Am.*, Vol. 93, pp. 3117–3127, 1993.

[4] M. V. Trevorrow. Measurements of near-surface bubble plumes in the open ocean with implications for high-frequency sonar performance. *J. Acoust. Soc. Am.*, Vol. 114, pp. 2672–2684, 2003.

[5] T. G. Leighton and G. B. N. Robb. Preliminary mapping of void fractions and sound speeds in gassy marine sediments from subbottom profiles. *J. Acoust. Soc. Am.*, Vol. 124, No. 5, pp. EL313–EL320, 2008.

[6] E. L. Carstensen and L. L. Foldy. Propagation of sound through a liquid containing bubbles. *J. Acoust. Soc. Am.*, Vol. 19, pp. 481–501, 1947.

[7] L. L. Foldy. The multiple scattering of waves. i. general theory of isotropic scattering by randomly distributed scatterers. *Phys. Rev.*, Vol. 67, pp. 107–119, 1945.

[8] F. E. Fox, S. R. Curley, and G. S. Larson. Phase velocity and absorption measurements in water containing air bubbles. *J. Acoust. Soc. Am.*, Vol. 27, No. 3, pp. 534–539, 1955.

[9] F. S. Crawford. The hot chocolate effect. *Am. J. Phys.*, Vol. 50, No. 5, pp. 398–404, 1982.

[10] G. Planinšič and E. Etkina. Bubbles that change the speed of sound. *Phys. Teach.*, Vol. 50, pp. 458–460, 2012.

[11] D. A. Drew. Mathematical modelling of two-phase flow. *Annu. Rev. Fluid Mech.*, Vol. 15, pp. 261–291, 1983.

[12] L. Rayleigh. On the pressure developed in a liquid during the collapse of a spherical cavity. *Phil. Mag.*, Vol. 34, pp. 94–98, 1917.

[13] M. S. Plesset. The dynamics of cavitation bubbles. *J. Appl. Mech.*, Vol. 16, pp. 227–282, 1949.

[14] H. Poritsky. The collapse or growth of a spherical bubble or cavity in a viscous fluid. *Proc. First Nat. Cong. in Appl. Math.*, pp. 813–821, 1952.

[15] C. Herring. Theory of the pulsations of the gas bubble produced by an underwater explosion. *OSRD Rep.*, No. 236, 1941.

[16] L. Trilling. The collapse and rebound of a gas bubble. *J. Appl. Phys.*, No. 23, pp. 14–17, 1952.

[17] J. B. Keller and I. I. Kolodner. Damping of underwater explosion bubble oscillations. *J. Appl. Phys.*, Vol. 27, pp. 1152–1161, 1956.

[18] J. B. Keller and M. Miksis. Bubble oscillations of large amplitude. *J. Acoust. Soc. Am.*, Vol. 68, pp. 628–633, 1980.

[19] A. Prosperetti and A. Lezzi. Bubble dynamics in a compressible liquid. part 1. first-order theory. *J. Fluid Mech.*, Vol. 168, pp. 457–478, 1986.

[20] A. Lezzi and A. Prosperetti. Bubble dynamics in a compressible liquid. part 2. second-order theory. *J. Fluid Mech.*, Vol. 185, pp. 289–321, 1987.

[21] S. Fujikawa and T. Akamatsu. Effects of the non-equilibrium condensation of vapour on the pressure wave produced by the collapse of a bubble in a liquid. *J. Fluid Mech.*, Vol. 97, pp. 481–512, 1980.

[22] A. Prosperetti, L. A. Crum, and K. W. Commander. Nonlinear bubble dynamics. *J. Acoust. Soc. Am.*, Vol. 83, No. 2, pp. 502–514, 1988.

[23] M. Kameda, M. Yamada, and Y. Matsumoto. Motion of a spherical gas bubble in an oscillatory pressure field. *Trans. Jpn. Soc. Mech. Eng. B*, Vol. 64, No. 622, pp. 1650–1658, 1998.

[24] M. Kameda and Y. Matsumoto. Nonlinear oscillation of a spherical gas bubble in acoustic fields. *J. Acoust. Soc. Am.*, Vol. 106, No. 6, pp. 3156–3166, 1999.

[25] A. Shima. The natural frequencies of two spherical bubbles oscillating in water. *J. Basic Engng., Trans. ASME*, Vol. 93, pp. 426–432, 1971.

[26] M. Morioka. Theory of natural frequencies of two pulsating bubbles in infinite liquid. *J. Nucl. Sci. Technol.*, Vol. 11, pp. 554–560, 1974.

[27] A. E. Wraith and T. Kakutami. The pressure beneath a growing rising bubble. *Chem. Eng. Sci.*, Vol. 29, pp. 1–12, 1974.

[28] S. Fujikawa and H. Takahira. Dynamics of two nonspherial cavitation bubbles in liquids. *Fluid Dyn. Res.*, Vol. 4, pp. 179–194, 1988.

[29] H. Takahira, T. Akamatsu, and S. Fujikawa. Dynamics of a cluster of bubbles in a liquid: theoretical analysis. *JSME Int. J. B*, Vol. 37, No. 2, pp. 297–305, 1994.

[30] H. Takahira. A remark on the pressure terms in the rayleigh-plesset equation for cavitating flows. *Trans. Jpn. Soc. Mech. Eng. B*, Vol. 70, No. 691, pp. 617–622, 2004.

[31] H. Takahira, T. Akamatsu, and S. Fujikawa. Dynamics of a cluster of bubbles in a liquid (2nd report, numerical analysis). *Trans. Jpn. Soc. Mech. Eng. B*, Vol. 58, No. 548, pp. 1275–1282, 1992.

[32] M. Watanabe and A. Prosperetti. Dynamic simulation of the acoustic characteristics of bubble clouds (1st report, construction of mathematical model). *Trans. Jpn. Soc. Mech. Eng. B*, Vol. 69, No. 688, pp. 2612–2619, 2003.

[33] M. Watanabe and A. Prosperetti. Dynamic simulation of the acoustic characteristics of bubble clouds (2st report, on validity of continuum mathematical model). *Trans. Jpn. Soc. Mech. Eng. B*, Vol. 70, No. 691, pp. 636–643, 2004.

[34] R. Egashira, T. Fujikawa, and S. Fujikawa. Interaction among straightly in-line spherical and unequal constant-volume bubbles moving with different velocities in liquid. *Trans. Jpn. Soc. Mech. Eng. B*, Vol. 78, No. 793, pp. 1534–1538, 2012.

[35] S. Fujikawa and H. Takahira. A theoretical study on the interaction between two spherical bubbles and radiated pressure waves in a liquid. *Acustica*, Vol. 61, pp. 188–199, 1986.

[36] H. Takahira, S. Fujikawa, and T. Akamatsu. Numerical investigation of nonlinear oscillations of two spherical gas bubbles in a compressible liquid. *JSME Int. J. II*, Vol. 32, No. 2, pp. 163–172, 1989.

[37] H. Takahira, S. Yamane, and T. Akamatsu. Nonlinear oscillations of a cluster of bubbles in a sound field (bifurcation structure). *JSME Int. J. B*, Vol. 38, pp. 432–439, 1995.

[38] A. Konno, H. Kato, H. Yamaguchi, and M. Maeda. On the collapsing behavior of cavitation bubble clusters. *JSME Int. J. B*, Vol. 45, pp. 631–637, 2002.

[39] L. van Wijngaarden. On the equations of motion for mixtures of liquid and gas bubbles. *J. Fluid Mech.*, Vol. 33, pp. 465–474, 1968.

[40] L. van Wijngaarden. One-dimensional flow of liquids containing small gas bubbles. *Annu. Rev. Fluid Mech.*, Vol. 4, pp. 369–396, 1972.

[41] L. Noordzij and L. van Wijngaarden. Relaxation effects, caused by relative motion, on shock waves in gas-bubble/liquid mixtures. *J. Fluid Mech.*, Vol. 66, pp. 115–143, 1974.

[42] R. E. Caflisch, M. J. Miksis, G. C. Papanicolaous, and L. Ting. Effective equations for wave propagation in bubbly liquids. *J. Fluid Mech.*, Vol. 153, pp. 259–273, 1985.

[43] K. W. Commander and A. Prosperetti. Linear pressure waves in bubbly liquids: Comarison between theory and experiments. *J. Acoust. Soc. Am.*, Vol. 85, pp. 732–746, 1989.

[44] D. Z. Zhang and A. Prosperetti. Ensemble phase-averaged equations for bubbly flows. *Phys. Fluids.*, Vol. 6, pp. 2956–2970, 1994.

[45] D. Z. Zhang and A. Prosperetti. Averaged equations for inviscid disperse two-phase flow. *J. Fluid Mech.*, Vol. 267, pp. 185–219, 1994.

[46] M. Watanabe and A. Prosperetti. Shock waves in dilute bubbly liquids. *J. Fluid Mech.*, Vol. 274, pp. 349–381, 1994.

[47] R. Egashira, T. Yano, and S. Fujikawa. Linear wave propagation of fast and slow modes in mixtures of liquid and gas bubbles. *Fluid Dyn. Res.*, Vol. 34, pp. 317–334, 2004.

[48] T. Yano, R. Egashira, and S. Fujikawa. Linear analysis of dispersive waves in bubbly flows based on averaged equations. *J. Phys. Soc. Jpn.*, Vol. 75, No. 10, p. 104401, 2006.

[49] T. Colonius, R. Hagmeijer, K. Ando, and C. E. Brennen. Statistical equilibrium of bubble oscillations in dilute bubbly flows. *Phys. Fluids*, Vol. 20, No. 4, p. 040902, 2008.

[50] K. Ando, T. Colonius, and C. E. Brennen. Numerical simulation of shock propagation in a polydisperse bubbly liquid. *Int. J. Multiphase Flow*, Vol. 37, pp. 596–608, 2011.

[51] T. Kanagawa, T. Yano, M. Watanabe, and S. Fujikawa. Unified theory based on parameter scaling for derivation of nonlinear wave equations in bubbly liquids. *J. Fluid Sci. Technol.*, Vol. 5, No. 3, pp. 351–369, 2010.

[52] T. Kanagawa, T. Yano, M. Watanabe, and S. Fujikawa. Nonlinear wave equation for ultrasound beam in nonuniform bubbly liquids. *J. Fluid Sci. Technol.*, Vol. 6, No. 2, pp. 279–290, 2011.

[53] T. Kanagawa, M. Watanabe, T. Yano, and S. Fujikawa. Nonlinear wave equations for pressure wave propagation in liquids containing gas bubbles (comparison between two-fluid model and mixture model). *J. Fluid Sci. Technol.*, Vol. 6, No. 6, pp. 838–850, 2011.

[54] T. Kanagawa. Two types of nonlinear wave equations for diffractive beams in bubbly liquids with nonuniform bubble number density. *J. Acoust. Soc. Am.*, Vol. 137, No. 5, pp. 2642–2654, 2015.

[55] D. Fuster and T. Colonius. Modelling bubble clusters in compressible liquids. *J. Fluid Mech.*, Vol. 688, pp. 352–389, 2011.

[56] D. Fuster, J. M. Conoir, and T. Colonius. Effect of direct bubble-bubble interactions on linear-wave propagation in bubbly liquids. *Phys. Rev. E*, Vol. 90, p. 063010, 2014.

[57] K. Ando, T. Sanada, K. Inaba, J. S. Damaso, J. E. Shepherd, T. Colonius, and C. E. Brennen. Shock propagation through a bubbly liquid in a deformable tube. *J. Fluid Mech.*, Vol. 671, pp. 339–363, 2011.

[58] K. Baik, T. G. Leighton, and J. Jiang. Investigation of a method for real time quantification of gas bubbles in pipelines. *J. Acoust. Soc. Am.*, Vol. 136, No. 2, pp. 502–513, 2014.

[59] M. Kameda and Y. Matsumoto. Shock waves in a liquid containing small gas bubbles. *Phys. Fluids*, Vol. 8, pp. 322–335, 1996.

[60] M. Kameda, N. Shimaura, F. Higashino, and Y. Matsumoto. Shock waves in a uniform bubbly flow. *Phys. Fluids*, Vol. 10, pp. 2661–2668, 1998.

[61] T. G. Leighton, K. Baik, and J. Jiang. The use of acoustic inversion to estimate the bubble size distribution in pipelines. *Proc. R. Soc. A*, Vol. 468, pp. 2461–2484, 2012.

[62] T. G. Leighton, J. Jiang, and K. Baik. Demonstration comparing sound wave attenuation inside pipes containing bubbly water and water droplet fog. *J. Acoust. Soc. Am.*, Vol. 131, No. 3 Pt 2, pp. 2413–2421, 2012.

[63] S. Matsukuma, W. Nishi, T. Ogasawara, and H. Takahira. Experimental investigations of pressure wave propagation by the inception of a laser-induced bubble in bubbly flows. *Jpn. J. Multiphase Flow*, Vol. 26, pp. 577–585, 2013.

[64] A. Minato. Numerical analysis of gas-liquid two-phase flow by using compressible two-fluid model. *Trans. Jpn. Soc. Mech. Eng. B*, Vol. 68, pp. 2489–2495, 2002.

[65] K. Ohtani, H. Sugiyama, and K. Mizobata. Large-amplitude shock wave propagation and bubble collapse in a water containing gas bubbles. *Trans. Jpn. Soc. Mech. Eng. B*, Vol. 68, pp. 1646–1652, 2002.

[66] W. Wiedemair, Z. Tukovic, H. Jasak, D. Poulikakos, and V. Kurtcuoglu. Modeling the interaction of microbubbles: effects of proximity, confinement, and excitation amplitude. *Phys. Fluids*, Vol. 26, No. 6, p. 062106, 2014.

[67] A. Kaneko, Y. Nomura, S. Takagi, Y. Matsumoto, and Y. Abe. Bubble breakup phenomena in a venturi tube. *Trans. Jpn. Soc. Mech. Eng. B*, Vol. 78, pp. 207–217, 2012.

[68] S. Uesawa, A. Kaneko, Y. Nomura, and Y. Abe. Study on bubble breakup behavior in a venturi tube. *Multiphase Sci. Technol.*, Vol. 24, pp. 257–277, 2012.

[69] A. B. Wood. *A Textbook of Sound.* Macmillan, New York, 1930.

[70] A. Mallock. The damping of sound by frothy liquids. *Proc. Roy. Soc. A*, Vol. 84, pp. 391–395, 1910.

[71] C. E. Brennen. *Cavitation and Bubble Dynamics.* Oxford university, New York, 1995.

[72] T. G. Leighton. *The Acoustic Bubble.* Academic, London, 1994.

[73] P. S. Wilson. Low-frequency dispersion in bubbly liquids. *Acoust. Res. Lett. Online*, Vol. 6, pp. 188–194, 2005.

[74] P. S. Wilson and R. A. Roy. An audible demonstration of the speed of sound in bubbly liquids. *Am. J. Phys.*, Vol. 76, pp. 975–981, 2008.

[75] M. Tohyama. *Physics of Sound.* Corona, Tokyo, 2010.

[76] C. F. Delale, S. Nas, and G. Tryggvason. Direct numerical simulations of shock propagation in bubbly liquids. *Phys. Fluids*, Vol. 17, p. 121705, 2005.

[77] C. F. Delale and G. Tryggvason. Shock structure in bubbly liquids: comparison of direct numerical simulations and model equations. *Shock Waves*, Vol. 17, pp. 433–440, 2008.

[78] K. M. Lee, K. T. Hinojosa, M. S. Wochner, T. F. Argo IV, P. S. Wilson, and R. S. Mercier. Sound propagation in water containing large tethered spherical encapsulated gas bubbles with resonance frequencies in the 50 Hz to 100 Hz range. *J. Acoust. Soc. Am.*, Vol. 130, pp. 3325–3332, 2011.

[79] K. Niki, Y. Jinbo, and H. Takahira. The two-dimensional direct numerical simulations of the propagation of pressure waves in gas-liquid two-phase flows

with the ghost fluid method. *Jpn. J. Multiphase Flow*, Vol. 25, pp. 459–467, 2012.

[80] J. H. Seo, S. K. Lele, and G. Tryggvason. Investigation and modeling of bubble-bubble interaction effect in homogeneous bubbly flows. *Phys. Fluids*, Vol. 22, p. 063302, 2010.

[81] V. E. Dontsov. Propagation of pressure waves in a gas-liquid medium with a cluster structure. *J. Appl. Mech. Tech. Phys.*, Vol. 46, pp. 346–354, 2005.

[82] P. S. Wilson, R. A. Roy, and W. M. Carey. Phase speed and attenuation in bubbly liquids inferred from impedance measurements near the individual bubble resonance frequency. *J. Acoust. Soc. Am.*, Vol. 117, pp. 1895–1910, 2005.

[83] M. Minnaert. On musical air-bubbles and the sounds of running water. *Philos. Mag.*, Vol. 16, pp. 235–248, 1933.

[84] M. Kafesaki, R. S. Penciu, and E. N. Economou. Air bubbles in water: a strongly multiple scattering medium for acoustic waves. *Phys. Rev. Lett.*, Vol. 84, pp. 6050–6053, 2000.

[85] R. P. Feynman, R. B. Leighton, and M. Sands. *The Feynman Lectures on Physics*, vol. 1. Addison-Wesley, Reading, MA, 1963.

[86] V. Leroy, A. Strybulevych, M. G. Scanlon, and J. H. Page. Transmission of ultrasound through a single layer of bubbles. *Eur. Phys. J. E*, Vol. 29, pp. 123–130, 2009.

[87] K. Yasui, Y. Iida, T. Tuziuti, T. Kozuka, and A. Towata. Strongly interacting bubbles under an ultrasonic horn. *Phys. Rev. E*, Vol. 77, p. 016609, 2008.

[88] H. Takahira. Comments on the technical terms for cavitation and bubble dynamics. *Jpn. J. Multiphase Flow*, Vol. 11, No. 1, pp. 66–69, 1997.

[89] A. Shima and T. Fujiwara. The behavior of two bubbles near a solid wall. *Archive of Appl. Mech.*, Vol. 62, No. 1, pp. 53–61, 1992.

[90] Y. Tomita, K. Sato, and A. Shima. Theoretical and experimental investigations on the nonspherical motion of a bubble near a plane rigid wall. *Trans. Jpn. Soc. Mech. Eng. B*, Vol. 59, No. 562, pp. 1891–1899, 1993.

[91] A. Shima. Dynamics of multiple bubbles. *Jpn. J. Multiphase Flow*, Vol. 8, No. 1, pp. 3–13, 1994.

[92] S. N. Domenico. Acoustic wave propagation in air-bubble curtains in water-part i: history and theory. *Geophysics*, Vol. 47, pp. 345–353, 1982.

[93] O. A. Druzhinin, L. A. Ostrovsky, and A. Prosperetti. Low-frequency acoustic wave generation in a resonant bubble layer. *J. Acoust. Soc. Am.*, Vol. 100, pp. 3570–3580, 1996.

[94] S. Karpov, A. Prosperetti, and L. Ostrovsky. Nonlinear wave interactions in bubble layers. *J. Acoust. Soc. Am.*, Vol. 113, No. 3, pp. 1304–1316, 2003.

[95] V. S. Surov. Interaction of a shock wave with a bubble screen. *Tech. Phys.*, Vol. 44, pp. 37–43, 1999.

[96] E. I. Timofeev, B. E. Gel'fand, A. G. Gumerov, M. M. Kofman, A. N. Polenov, and S. V. Khomik. Influence of a bubble screen on shock-wave perturbation in a fluid. *Combustion, Explosion, and Shock Waves*, Vol. 21, pp. 361–365, 1985.

[97] K. Kobayashi. *Physics of Light: Why is light refracted, reflected and scattered?* University of Tokyo Press, Tokyo, 2002.

Acknowledgements

The author wishes to acknowledge indebtedness to Professor Masao Watanabe and Associate Professor Kazumichi Kobayashi of Hokkaido University. Without their sharp suggestions and continued encouragements, the present study cannot be accomplished.

The present study has been financially supported from Japan Society for the Promotion of Science, Research Fellowship for Young Scientists (No. 26·1417). The author would like to express his deepest gratitude toward this grant.